CHAPTER 4 RESULTS AND DISCUSSIONS

In this Chapter, the results of physical model test on small-scale reinforce and unreinforced polymer modified asphalt pavements in laboratory applied with cyclic load were presented. Different deformation characteristic and strain distribution of unreinforced and reinforced polymer modified asphalt pavements were described and discussed. Also, different results by different types of asphalt cement were compared.

4.1 Parameters and Definition

A pressure, which is transferred to the model footing, can be calculated following Equation 4.1.

$$p = \frac{L}{A} \tag{4.1}$$

where: p = Footing pressure (kPa)
L = Axial loading (kN)
A = Cross-section area of footing (m^2)

Figure 4.1 shows the definition of the number of cyclic loading and permanent deformation. From the beginning of testing, cyclic load, which was started from 0 kPa and increased to 400 kPa, is treated as the first cycle (N_c = 1). Then, the second cycle (N_c = 2) was continuously started from the first cycle, by decreasing to 10 kPa and increasing to 400 kPa. The differential deformation from the first and the second cycle was permanent deformation developed by the second cycle.

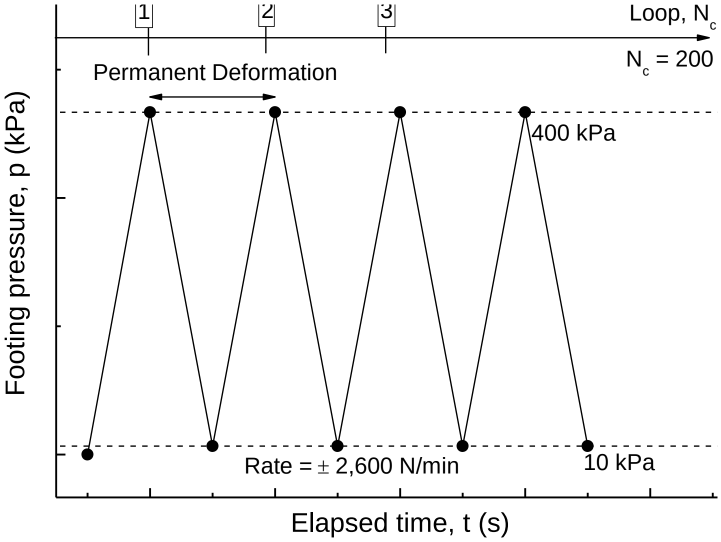

Figure 4.1 Relationship between footing pressure and elapsed time of testing and definition of the number of cyclic loading and permanent deformation

The fabric effectiveness factor (FEF) can be calculated from Equation 4.2.

$$FEF = \frac{\delta_n}{\delta_r} \qquad (4.2)$$

where: δ_n = Permanent deformation of footing at N_c = 200 for unreinforced case (mm)

δ_r = Permanent deformation of footing at N_c = 200 for reinforced case (mm)

The covering ratio (CR) can be calculated from the following:

$$CR = \frac{A_{Geosynthetics}}{A_{All}} \times 100\% \qquad (4.3)$$

where: $A_{Geosynthetics}$ = Projected area of geosynthetic on a plane of pavement (cm^2)

A_{All} = Area of pavement (cm^2)

4.2 New Unreinforced and Overlayed Unreinforced Polymer Modified Asphalt (PMA) Pavement

4.2.1 Footing settlement and Footing Permanent Settlement

The preparations of new and overlayed PMA pavements were different by the specified densities (Section 3.4.2). For new pavement, the specified density was 2.1 g/cm^3. But, the specified density for overlayed pavement was 1.8 g/cm^3 for old pavement in the bottom half and 2.1 g/cm^3 for new pavement in the top half.

Figure 4.2(a) compares the relationship between the footing pressure and the footing settlement for new and overlayed PMA pavements. The footing pressures were calculated from Equation 4.1 and the footing settlement were measured from a sensor, which was installed at the center of the model footing. Figure 4.2(b) compares the relationship between the footing settlement and the elapsed time for new and overlayed PMA pavements and Figure 4.2(c) compares the relationship between a permanent settlement of footing and a number of cycles of cyclic loading for new and overlayed PMA pavements. The permanent settlements of footing were as described above. The following trends of behavior may be seen from Figure 4.2(a)-Figure 4.2(c):

1) Both the footing settlement and the footing permanent settlement increased with an increase in the number of cycles of cyclic loading, the footing pressure and the elapsed time.
2) The rate of footing permanent settlement development decreased with an increase in the number of cycles of cyclic loading. That is, the footing permanent settlement was relatively grately occurred in the first section of loading (approximately N_c = 1 to N_c = 50). During this period, it seems that additional densification of the pavement structure achived. After that, the footing permanent settlement was less occurred and was stable in the last section of loading. It seems, therefore, that the above-mentioned densification slowly decreased in this section.

3) The new PMA pavement (NPNO) showed a greater footing settlement and footing permanent settlement than those of the overlayed PMA pavement (DMNO).
4) On the other hand, the permanent settlement of footing development rate in the new PMA pavement (NPNO) exhibited a relatively less value that was equal to 0.01625 mm/cycle. And, the permanent settlement of footing development rate in the overlayed PMA pavement (DMNO) exhibited a relatively greater value that was equal to 0.0177 mm/cycle. The permanent settlement of footing development rate was calculated from the occurrence of permanent deformation in the last section of loading because the permanent footing settlement was less occurred and was rather stable. When comparing the performance of new and overlayed pavements, the new PMA pavement (NPNO) was more effective in this respect.

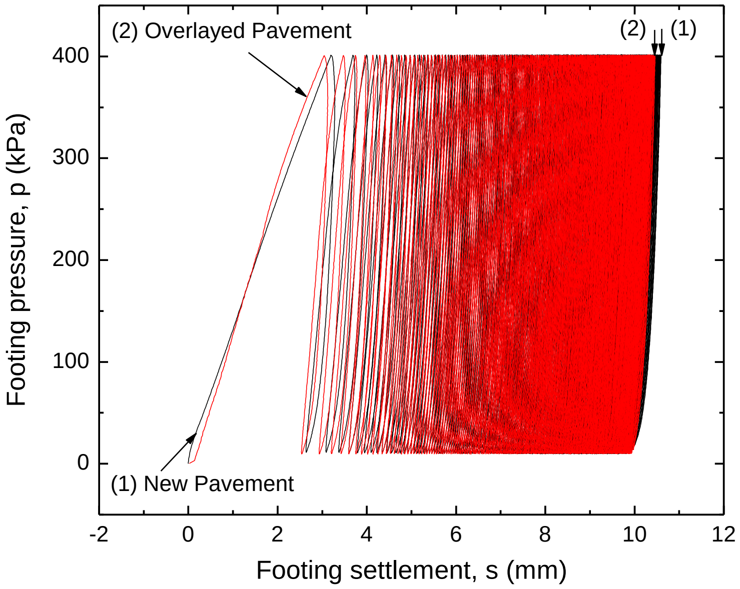

Figure 4.2(a) Relationship between footing pressure and footing settlement in new and overlayed polymer modified asphalt pavements

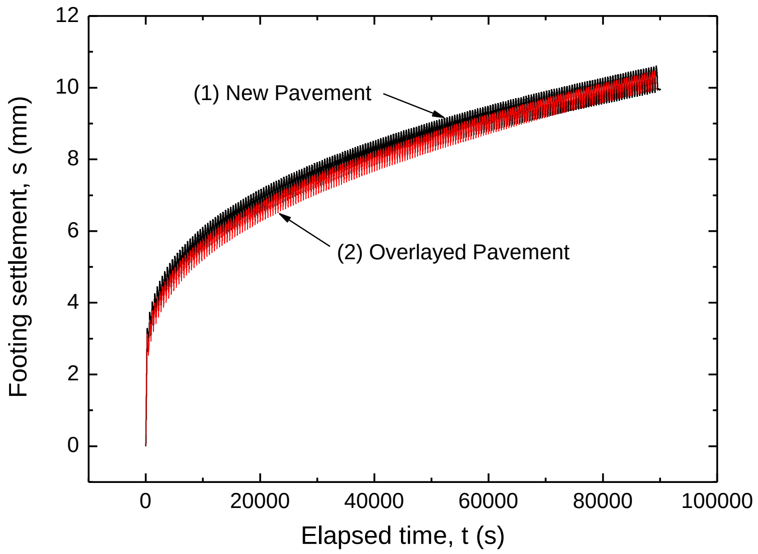

Figure 4.2(b) Relationship between footing settlement and elapsed time in new and overlayed polymer modified asphalt pavements

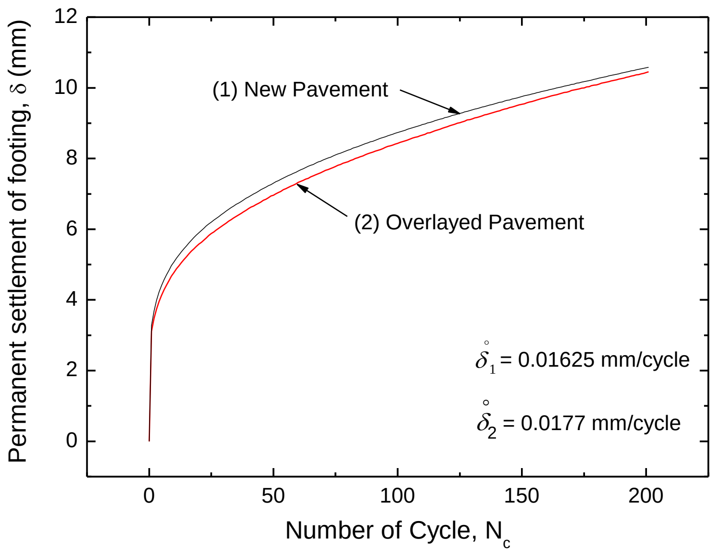

Figure 4.2(c) Relationship between permanent settlement of footing settlement and number of cycle in new and overlayed polymer modified asphalt pavements

4.2.2 Surface Settlement and Settlement Underneath Pavement

Figure 4.3(a) compares the relationship between the surface settlement and the distance from center of footing for different numbers of cycle for new and overlayed PMA pavements. There are four laser sensors for measurement of the surface settlement in this study. One sensor was used to measure the model footing settlement (Section 4.2.1) and the other three sensors to measure the surface settlement of the pavement at distance of 60 mm (1D), 150 mm (2.5D) and 300 mm (5D) from the center of model footing, respectively. D is width of footing model (60 mm). Figure 4.3(b) compares the settlement underneath polymer modified asphalt pavement for different number of cycles for new and overlayed PMA pavements. The settlements underneath polymer modified asphalt pavement were obtained by photogrametric analysis. These settlements were measured and analyzed from the first row of makers from the top of natural latex sheet, as shown in Figure 4.4. Thus, they were the settlements at the bottom of pavement. The following trends of behavior may be seen from Figure 4.3(a) and Figure 4.3(b):

1) Both the surface settlement and the settlement underneath polymer modified asphalt pavement increased with an increase in the numbers of cycle of cyclic loading.
2) On the other hand, both the surface settlement and the settlement underneath polymer modified asphalt pavement decreased with an increase in the distance from center of footing.
3) The new PMA pavement (NPNO) showed a greater surface settlement and settlement underneath pavement than those of overlayed PMA pavement (DMNO).
4) In the first section of loading (N_c = 5 and N_c = 10), the trend of surface settlement and settlement underneath pavement were similar new and overlayed PMA pavements. The direction of surface settlement and settlement underneath pavement were downward for both new and overlayed pavements in all the distress from the center. On the other hand, the trend of surface settlement and settlement underneath pavement was different in new and overlayed PMA pavement in the last section of loading (N_c = 190, N_c = 195 and N_c = 200). For new PMA pavement (NPNO), the direction of surface settlement and settlement underneath pavement were similar the ones during the first section of loading. For overlayed PMA pavement (DMNO), the direction of surface settlement and settlement underneath pavement were downward at center of footing and 60 mm from center of footing; it became upward at approximately 100 mm from center of footing.
5) From the above, stiffness in overlayed PMA pavement may be less than the one in new PMA pavement. That is, the low density of the bottom half of overlayed pavement resulted in the decrease of the overall pavement stiffness. Therefore, rigidity in overlayed PMA pavement was also less. The overlayed PMA pavement probably occurred to bend.

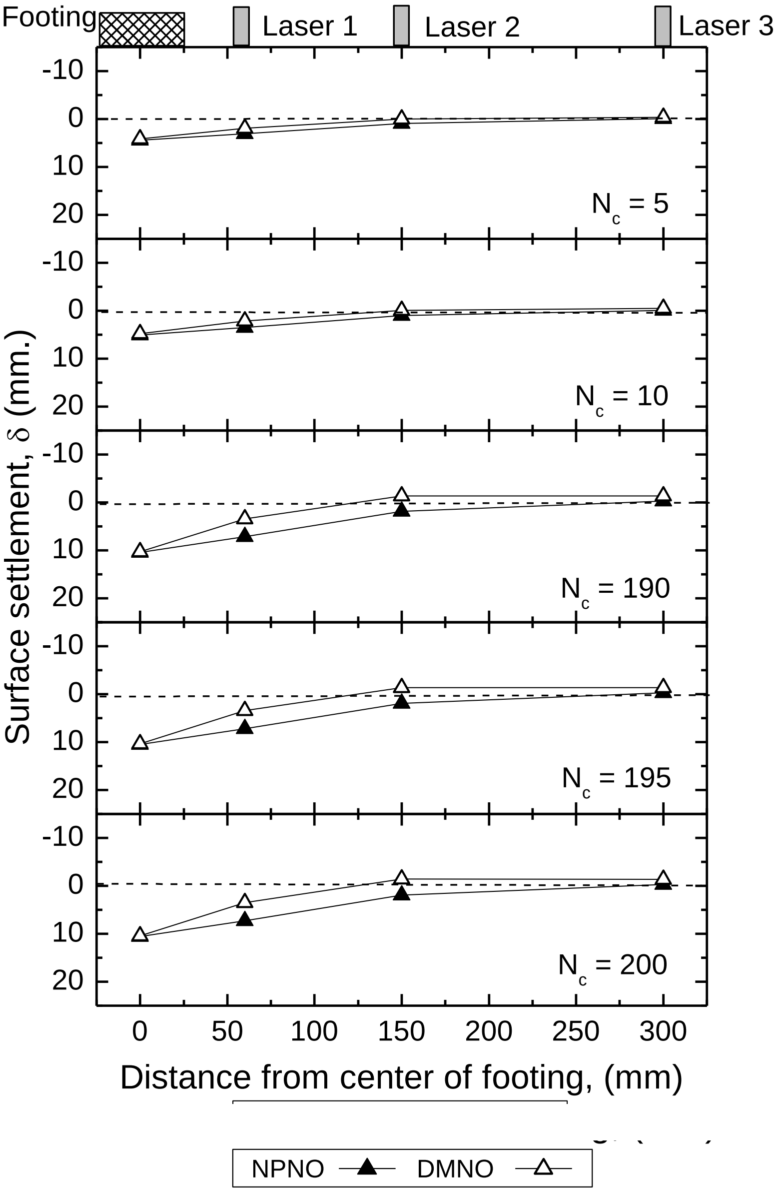

Figure 4.3(a) Relationship between surface settlement and distance from center of footing in new and overlayed polymer modified asphalt pavements

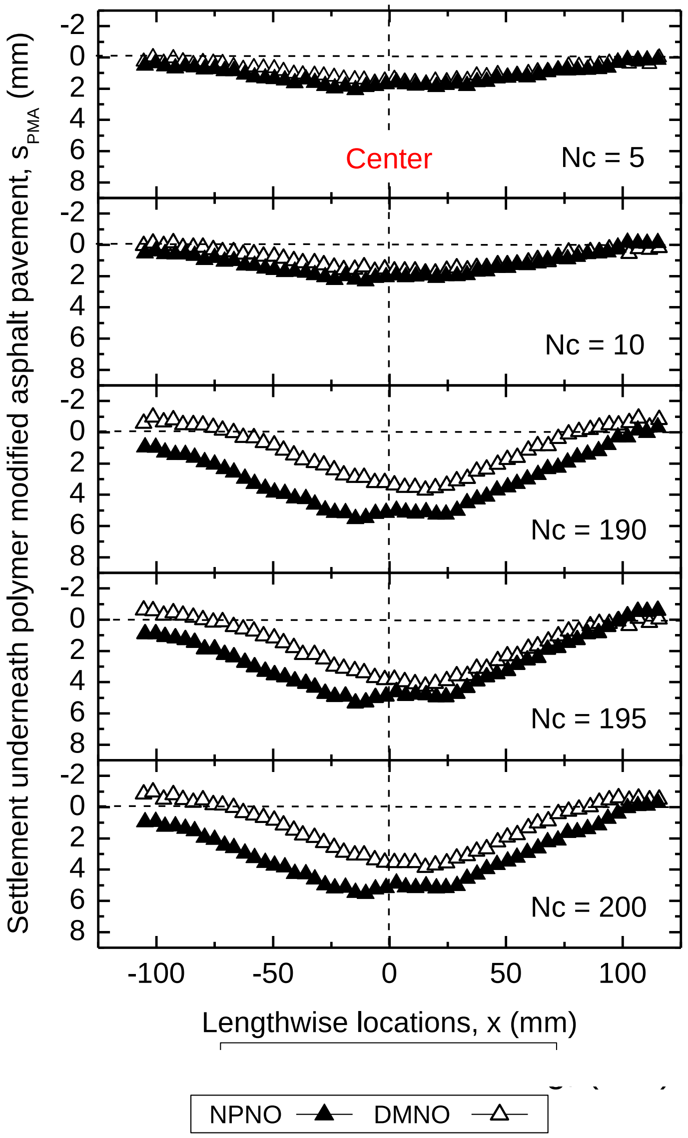

Figure 4.3(b) Settlement underneath polymer modified asphalt pavement in new and overlayed polymer modified asphalt pavements

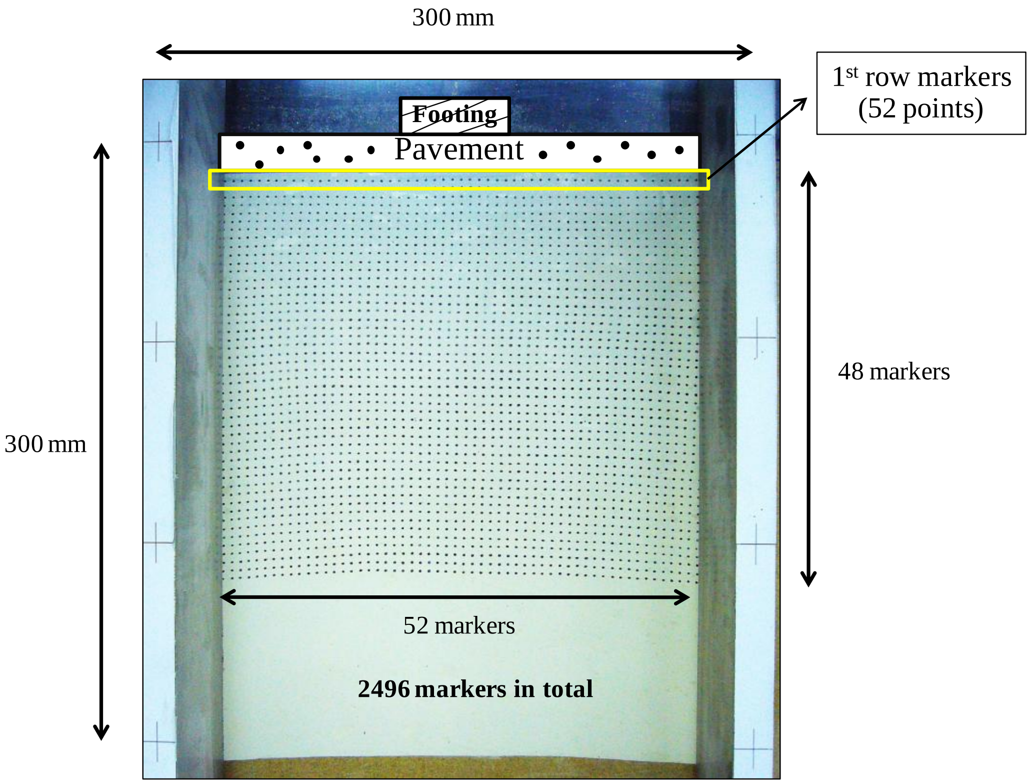

Figure 4.4 First row makers that were used for determination of the settlements underneath polymer modified asphalt pavement

4.2.3 Strain Field of Sand Subbase

A photogrametric analysis was used to determine the maximum shear strain distribution in the sand layer in this study. For calculating these strain values, source codes were newly written in MATLAB computer program (Kongkitkul, 2004). Three sets of source codes were written considering the different patterns of arrangement of element. The source code named "normal overlapping elements" was used in this study (Section 2.6.5).

Figure 4.5(a) shows the maximum shear strain ($\gamma_{\max}$) distribution in the new PMA pavement at 200 cycles of cyclic loading and Figure 4.5(b) shows maximum shear strain ($\gamma_{\max}$) distribution in the overlayed PMA pavement at 200 cycles of cyclic loading. Figure 4.5(c) shows relationship between average of $\gamma_{\max}$ and number of cycle in the new and the overlayed polymer modified asphalt pavements. The following trends of behavior may be seen from Figure 4.5(a)-Figure 4.5(c):

1) For the new and overlayed unreinforced PMA pavements, the new PMA pavement showed a greater maximum shear strain ($\gamma_{\max}$) distribution. The shear bands may be clearly seen in the new PMA pavement (NPNO) while it is not obvious for the overlayed PMA pavement.
2) The new PMA unreinforced pavement showed a greater rate of maximum shear strain ($\gamma_{\max}$) development, while the overlayed unreinforced PMA pavement showed a lower rate of maximum shear strain ($\gamma_{\max}$) development.

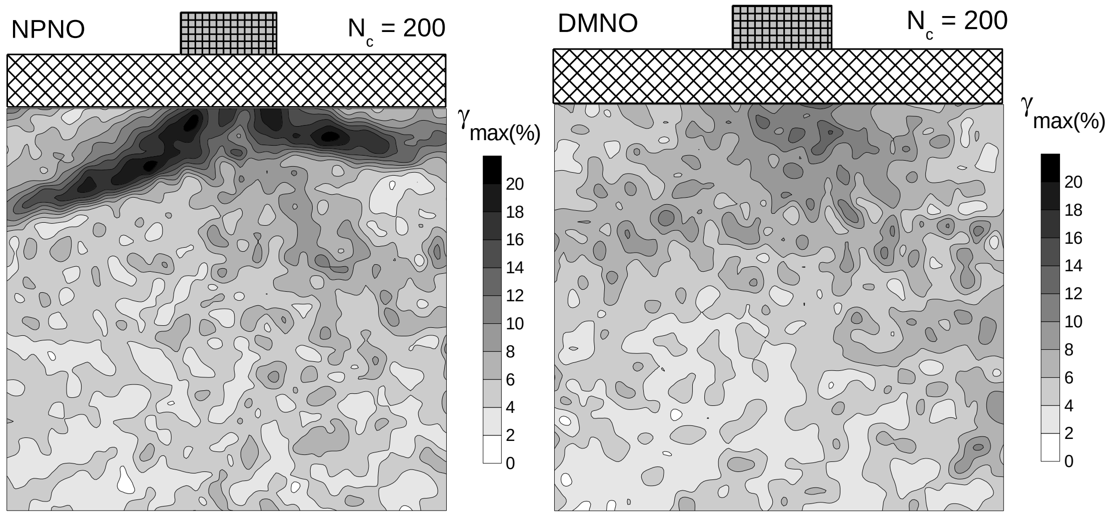

(a) (b)

Figure 4.5 Maximum shear strain distribution at 200 cycles of cyclic loading; (a) new pavement (NPNO) and (b) overlayed pavement (DMNO)

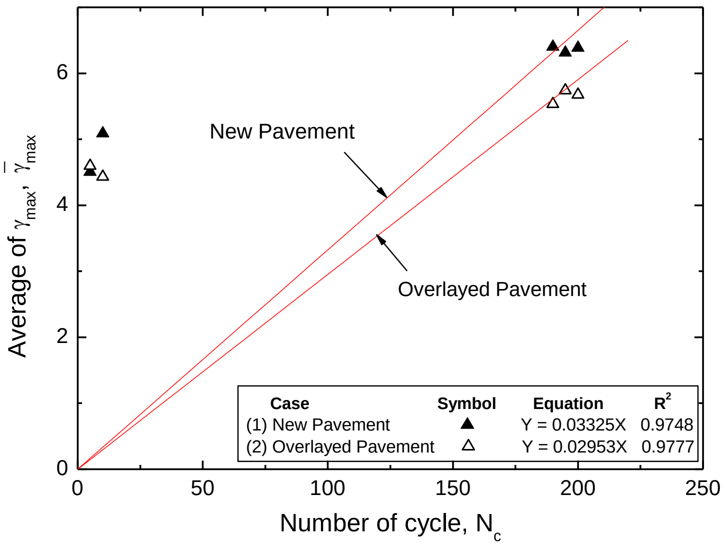

Figure 4.5(c) Relationship between average of $\gamma_{\max}$ and number of cycle in new and overlayed polymer modified asphalt pavements

4.2.4 Surface Cracking

After having completed tests, photos of pavement surface around the model footing were taken for observation of surface cracking. Then, the lines, drawn onto the photo by solid line, represented the potential surface cracking on pavement surface. And, a rectangular, drawn in photo by dash line, located the position of the model footing.

Figure 4.6 shows surface cracking in the new and the overlayed unreinforced polymer modified asphalt pavements. In the new pavement, three cracks were observed along the edge of model footing. On the other hand, surface cracking in overlayed pavement could not be observed, because the model pavement was broken while moving out from the container.

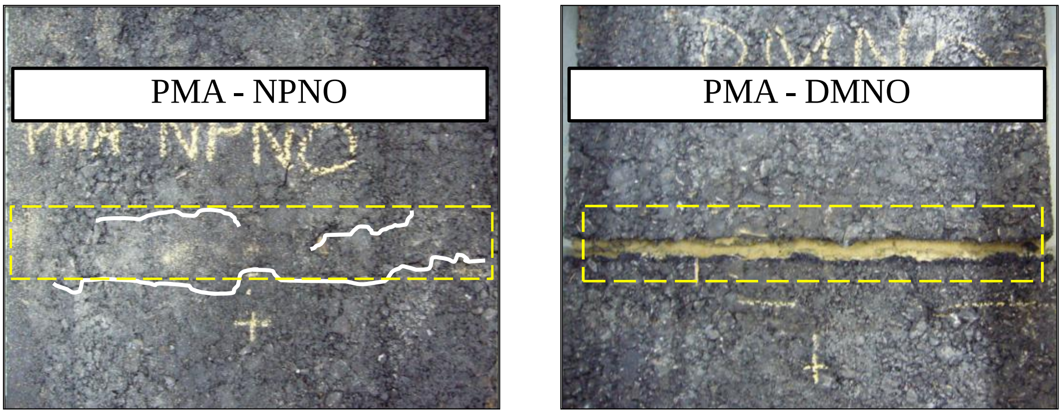

(a) (b)

Figure 4.6 Surface cracking in unreinforced polymer modified asphalt pavements: (a) new pavement (NPNO) and (b) overlayed pavement (DMNO)

4.3 New Unreinforced and New Reinforced Polymer Modified Asphalt Pavement

4.3.1 Footing settlement and Footing Permanent Settlement

Figure 4.7(a) compares the relationship between the footing pressure and the footing settlement for new unreinforced and new reinforced PMA pavements. Figure 4.7(b) compares the relationship between the footing settlement and the elapsed time for new unreinforced and new reinforced PMA pavements. Figure 4.7(c) compares the relationship between the permanent settlement of footing and the number of cycles of cyclic loading for new unreinforced and reinforced PMA pavements. The following trends of behavior may be seen from Figure 4.7(a)-Figure 4.7(c):

1) Both the footing settlement and the footing permanent settlement increased with an increase in the numbers of cycle of cyclic loading, the footing pressure and the elapsed time.
2) The permanent settlement of the footing significantly decreased with PMA pavement reinforced with geosynthetics; that is, the new unreinforced PMA pavement (NPNO) showed greater footing settlement than other cases. The new PMA pavement reinforced with geogrid together with geocomposite

(NPGGGT), new PMA pavement reinforced with geogrid (NPGG) and new reinforced PMA pavement with geocomposite (NPGT) respectively exhibited settlement from a greater to a lower value among the reinforced cases. It may be seen likely that reinforcing with geosynthetics in new PMA pavement can widely distribute pressure underneath model footing to a wider area underneath. Thus, the rigidity of pavement was increased by this reinforcing effect.

3) The rate of footing permanent settlement development decreased with an increase in the number of cycles of cyclic loading. That is, the footing permanent settlement relatively occurred in the first section of loading (approximately $N_c = 1$ to $N_c = 50$). This may be due to plastic deformations (irreversible deformation) which occurred in some area of pavement structure underneath footing model. After that, the footing permanent settlement relative less occurred and stable in the last section of loading. Due to occurring plastic deformation in the first section of loading, the plastic deformation was less distributed to new area of pavement structure.
4) The rate of footing permanent settlement development decreased with PMA pavement reinforced with geosynthetics. The footing permanent settlement rate in PMA pavement reinforced with geocomposite (NPGT) was the smallest value among new PMA pavement, equal to 0.00484 mm/cycle. The PMA pavement reinforced with geogrid (NPGG), PMA pavement reinforced with geogrid and geocomposite (NPGGGT) and unreinforced PMA pavement (NPNO) showed greater rates of footing permanent settlements that were equal to 0.00693, 0.00755 and 0.01625 mm/cycle, respectively.

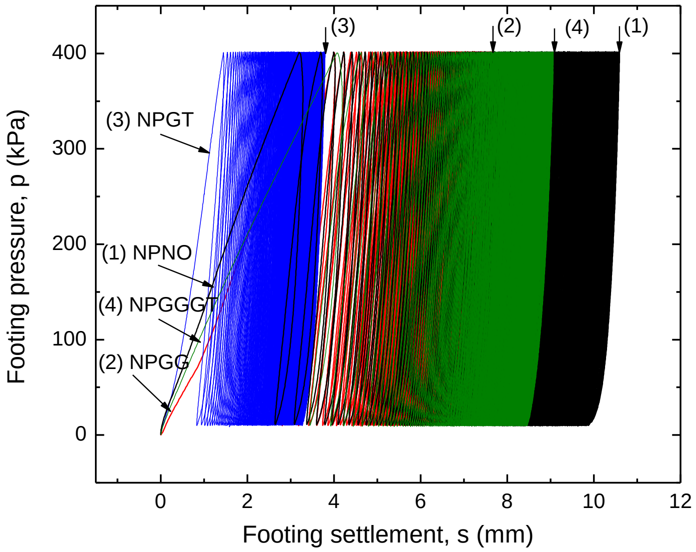

Figure 4.7(a) Relationship between footing pressure and footing settlement in new unreinforced and new reinforced polymer modified asphalt pavements

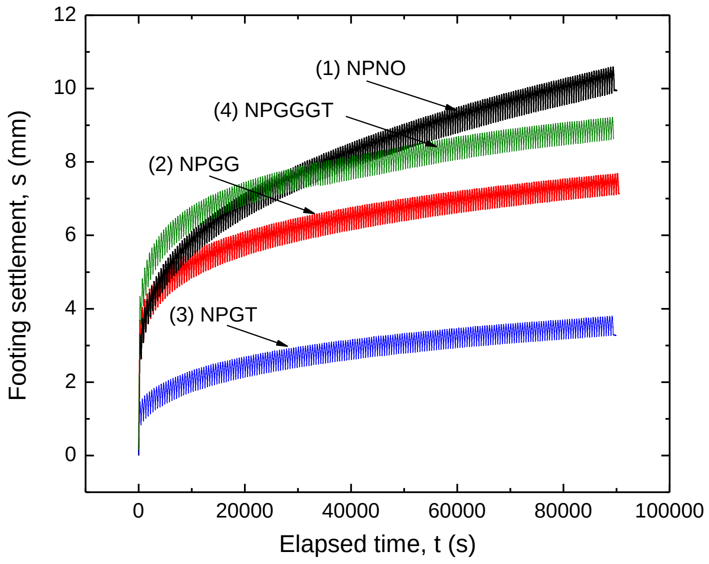

Figure 4.7(b) Relationship between footing settlement and elapsed time in new unreinforced and new reinforced polymer modified asphalt pavements

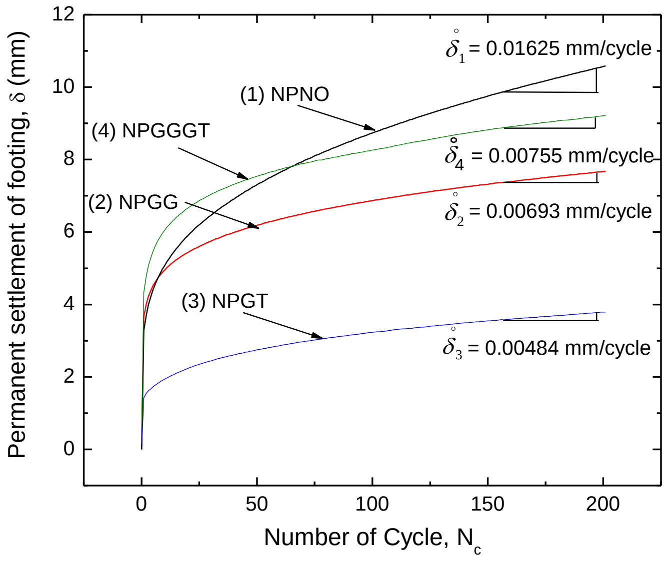

Figure 4.7(c) Relationship between permanent settlement of footing and number of cycle in new unreinforced and new reinforced polymer modified asphalt pavements

4.3.2 Surface Settlement and Settlement Underneath Pavement

Figure 4.8(a) compares the relationship between the surface settlement and the distance from center of footing at different number of cycle for new unreinforced and new reinforced PMA pavements. Figure 4.8(b) compares the settlement underneath polymer modified asphalt pavement at different number of cycle for new unreinforced and new reinforced PMA pavement. The following trends of behavior may be seen from Figure 4.8(a) and Figure 4.8(b):

1) Both the surface settlement and the settlement underneath polymer modified asphalt pavement increased with an increase in the number of cycles of cyclic loading.
2) On the other hand, both the surface settlement and the settlement underneath polymer modified asphalt pavement decreased with an increase in the distance from center of footing.
3) The surface settlement significantly decreased in new PMA pavement reinforced with geosynthetics. The new unreinforced PMA pavement (NPNO) showed a greater surface settlement. The new PMA pavement reinforced with geogrid together with geocomposite (NPGGGT), new PMA pavement reinforced with geogrid (NPGG) and new reinforced PMA pavement with geocomposite (NPGT) exhibited the surface settlement from a greater to a lower value, respectively.
4) The settlement underneath pavement significantly decreased with new PMA pavement reinforced with geosynthetics. The sequences of settlement were the same as those of surface settlement.
5) The trends of surface settlement and settlement underneath pavement were similar for both new unreinforced and reinforced PMA pavement in the first section of loading (N_c = 5 and N_c = 10) and the last section of loading (N_c = 190, N_c = 195 and N_c = 200). The direction of surface settlement and settlement underneath pavement were downward for all the distances from the center.
6) From the above, reinforcing in new PMA pavement with geosynthetics can improve rigidity of pavement. Thus, rutting, a distress type in pavement, was possibly decreased when reinforcing in new PMA pavement with geosynthetics.

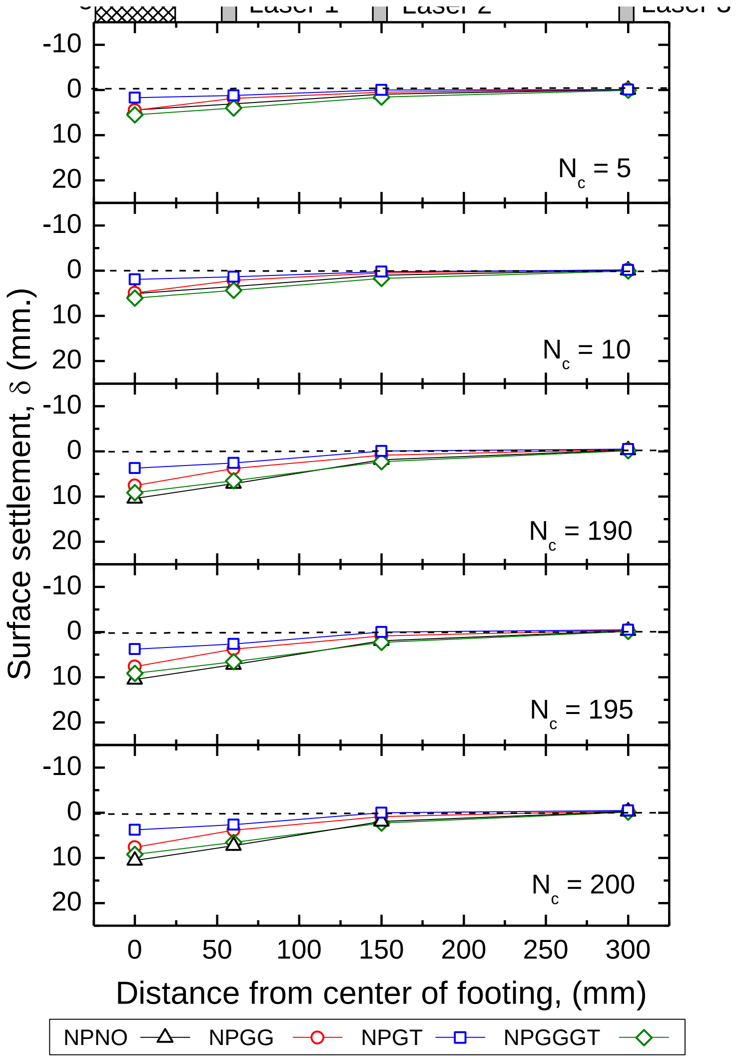

Figure 4.7(a) Relationship between surface settlement and distance from center of footing in new unreinforced and new reinforced polymer modified asphalt pavements

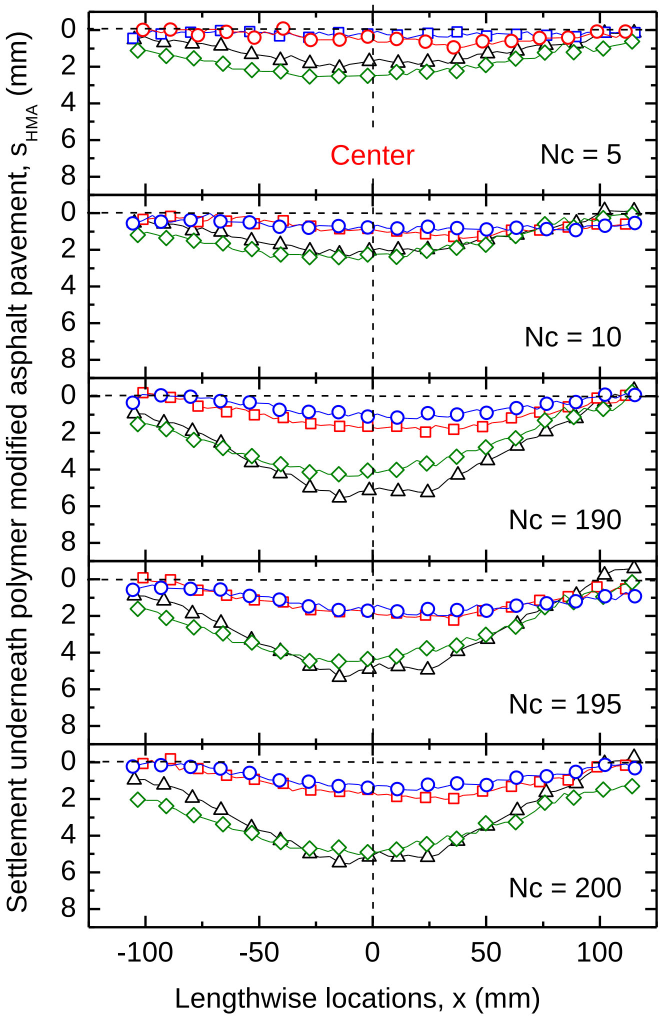

Figure 4.7(b) Settlement underneath polymer modified asphalt pavement in new unreinforced and new reinforced polymer modified asphalt pavements

4.3.3 Strain Field of Sand Subbase

Figure 4.9(a) shows maximum shear strain ($\gamma_{\max}$) distribution in new unreinforced PMA pavement at 200 cycles of cyclic loading. Figure 4.9(b) shows maximum shear strain ($\gamma_{\max}$) distribution in new PMA pavement reinforced with geogrid at 200 cycles of cyclic loading. Figure 4.9(c) shows maximum shear strain ($\gamma_{\max}$) distribution in new PMA pavement reinforced with geocomposite at 200 cycles of cyclic loading. Figure 4.9(d) shows maximum shear strain ($\gamma_{\max}$) distribution in new reinforced PMA pavement with geogrid together with geocomposite at 200 cycles of cyclic loading. Figure 4.9(e) shows shows relationship between the average of $\gamma_{\max}$ and number of cycle in new unreinforced and new reinforced polymer modified asphalt pavements. The following trends of behavior may be seen from Figure 4.9(a)-Figure 4.9(e):

1) A shear band can be clearly seen in the new unreinforced PMA pavement (NPNO) and noticeable in new PMA pavement reinforced with geogrid together with geocomposite (NPGGGT).
2) The maximum shear strain ($\gamma_{\max}$) distribution significantly decreased when reinforced PMA pavement with geosynthetics. The new unreinforced PMA pavement (NPNO) showed the greatest maximum shear strain ($\gamma_{\max}$) distribution. The new PMA pavement reinforced with geogrid together with geocomposite (NPGGGT), new reinforced PMA pavement with geogrid (NPGG) and new PMA pavement reinforced with geocomposite (NPGT) exhibited the maximum shear strain ($\gamma_{\max}$) from a greater to lower, respectively.
3) The rate of maximum shear strain ($\gamma_{\max}$) development significantly decreased when reinforced PMA pavement with geosynthetics. The new unreinforced PMA pavement (NPNO) showed the greatest rate of maximum shear strain ($\gamma_{\max}$) development value among new PMA pavements, equal to 0.03325 %/cycle. The new PMA pavement reinforced with geogrid together with geocomposite (NPGGGT), new reinforced PMA pavement with geogrid (NPGG) and new PMA pavement reinforced with geocomposite (NPGT) exhibited the rate of maximum shear strain ($\gamma_{\max}$) development from a greater to lower value that were equal to 0.02993, 0.02712 and 0.02575 %/cycle, respectively. Therefore, the maximum shear strain ($\gamma_{\max}$) may be the most occurred in new unreinforced PMA pavement (NPNO) among these new PMA pavements.
4) From the above, sand subbase failure may occurred along direction of shear band in the new unreinforced PMA pavement (NPNO) before the other three pavements (the new PMA pavement reinforced with geogrid together with geocomposite (NPGGGT), new PMA pavement reinforced with geogrid (NPGG) and new PMA pavement reinforced with geocomposite (NPGT)). From the results, reinforcing with geosynthetics in new PMA pavement can widely distribute pressure underneath model footing to a wider area underneath.

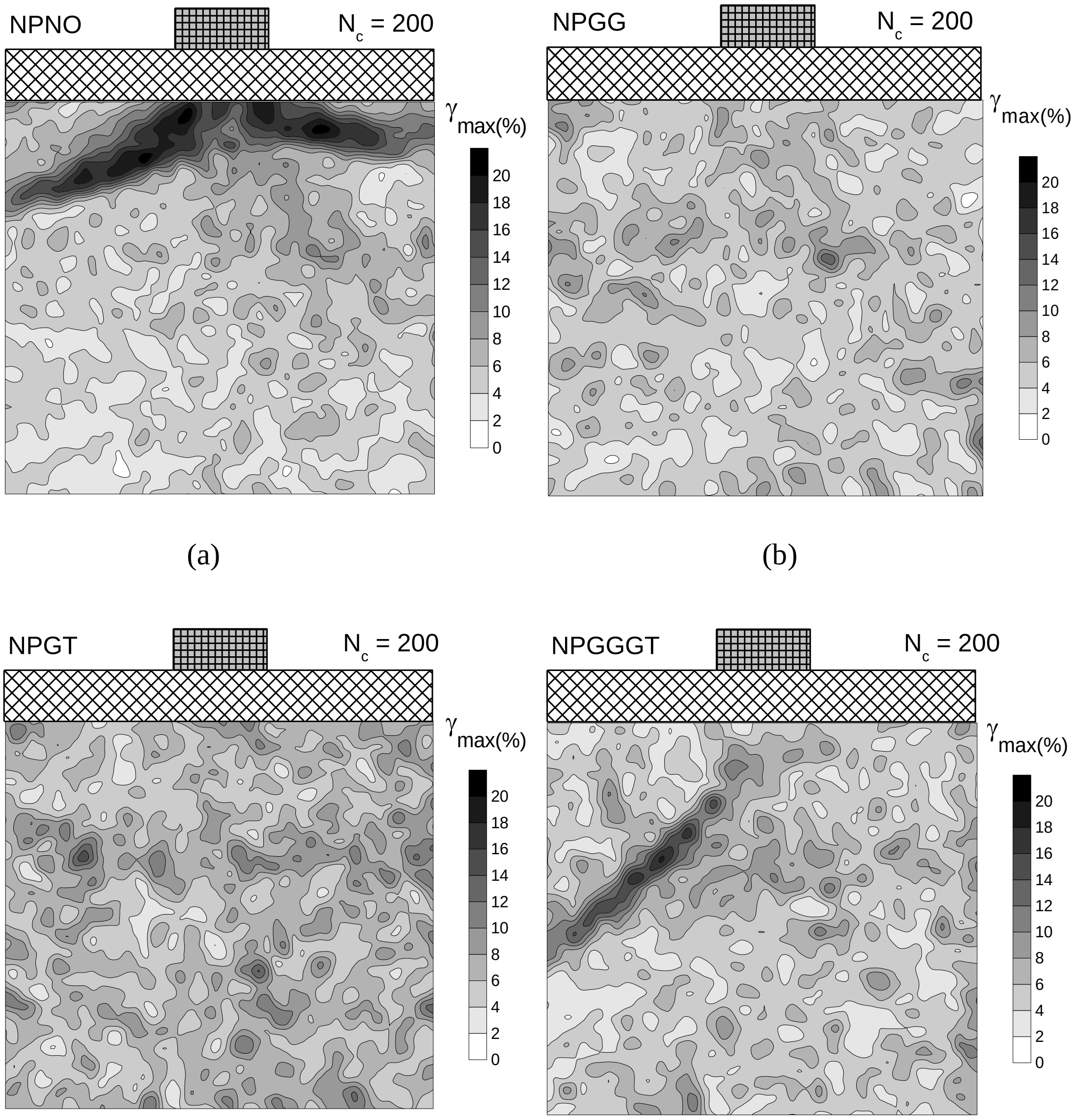

(a) (b)

(c) (d)

Figure 4.9 Maximum shear strain distribution at 200 cycles of cyclic loading; (a) new unreinforced PMA pavement (NPNO), (b) new PMA pavement reinforced with geogrid (NPGG), (c) new PMA pavement reinforced with geocomposite (NPGT) and (d) new PMA pavement reinforced with geogrid together with geocomposite (NPGGGT)

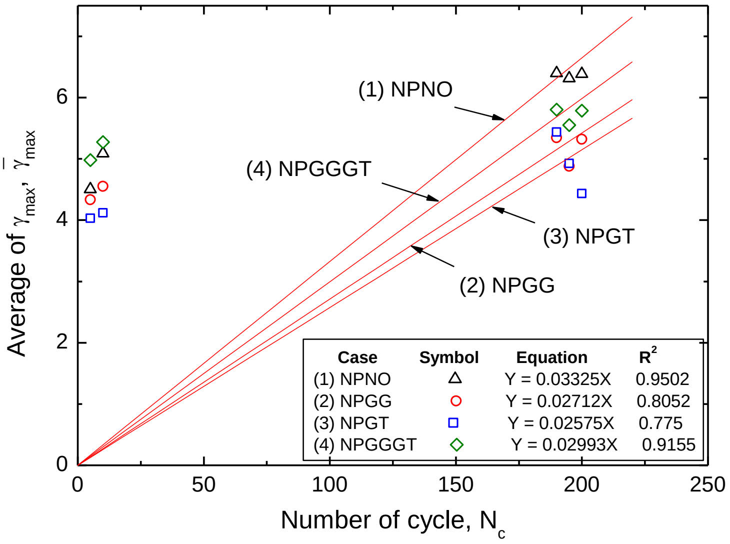

Figure 4.9(e) Relationship between the average of γ_{max} and number of cycle in new unreinforced and new reinforced polymer modified asphalt pavements

4.3.4 Surface Cracking

Figure 4.10 shows surface cracking in new unreinforced and new reinforced polymer modified asphalt pavements. The surface cracking decreased with PMA pavement reinforced with geosynthetics. The surface cracking in PMA pavement reinforced with geocomposite (NPGT) was the smallest seen among new PMA pavements. It showed only one crack in pavement. The PMA pavement reinforced with geogrid (NPGG), PMA pavement reinforced with geogrid and geocomposite (NPGGGT) and unreinforced PMA pavement (NPNO) showed greater degree of surface cracking, successively. And, the most of surface cracking may occurred around the edge of model footing. Therefore, reinforcing with geosynthetics in new PMA pavement could decrease surface cracking around area that wheel contacted onto pavement.

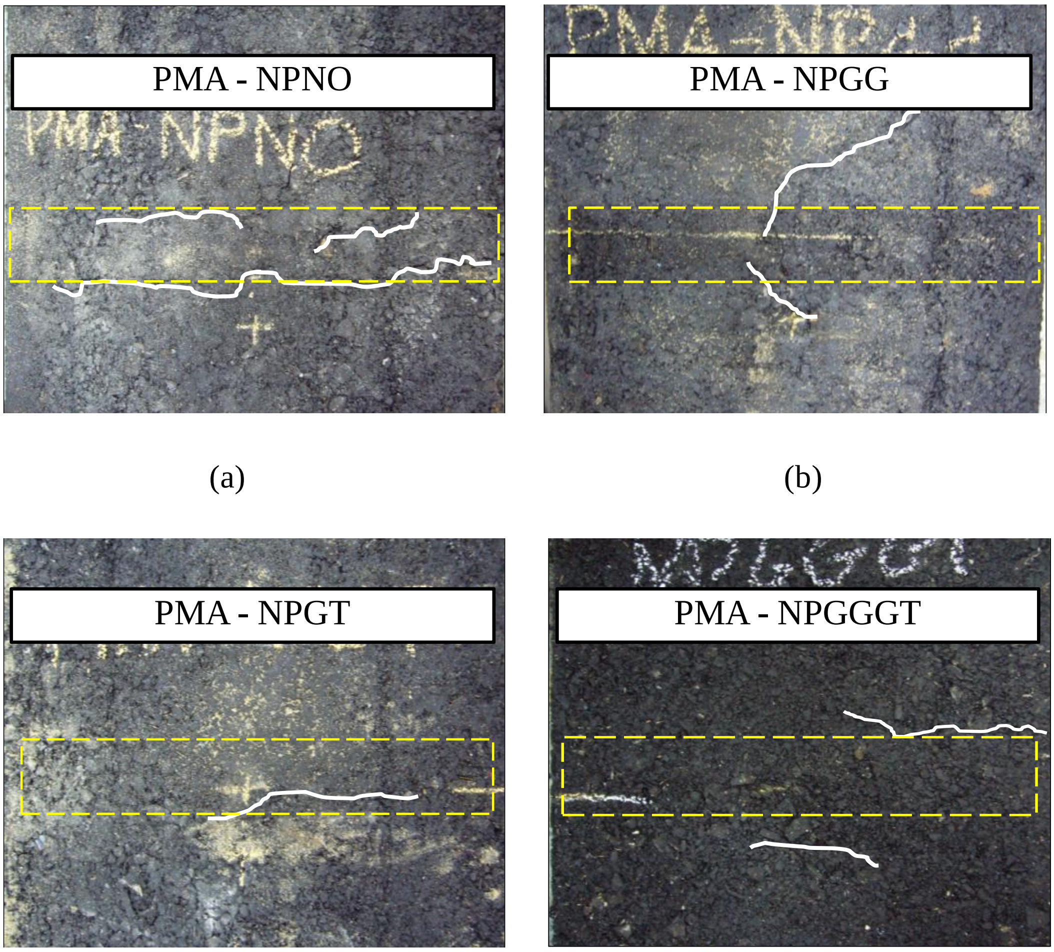

(a) (b)

(c) (d)

Figure 4.10 Surface cracking in polymer modified asphalt pavements; (a) new unreinforced PMA pavement (NPNO), (b) new PMA pavement reinforced with geogrid (NPGG), (c) new PMA pavement reinforced with geocomposite (NPGT) and (d) new PMA pavement reinforced with geogrid together with geocomposite (NPGGGT)

4.3.5 Fabric Effective Factor

The fabric effectiveness factor (FEF) of reinforced pavement can be determined from Equation 4.2. FEF value can be used and implemented into the design traffic number to determine the modified design traffic number value and design accordingly. Also, it was an important factor for selection of type of geosynthetics.

Table 4.1 shows FEF value for the new reinforced PMA pavements. FEF value for new PMA pavement reinforced with geocomposite (NPGT) showed the greatest value for new PMA pavements, equal to 2.79. The new PMA pavement reinforced with geogrid (NPGG) and new PMA pavement reinforced with geogrid together with geocomposite (NPGGGT) showed a less FEF value, equal to1.38 and 1.15, respectively. When comparing the performance among new reinforced PMA pavements, the PMA pavement reinforced with geocomposite (NPGT) was the most effective for this study. Thus, geocomposite was a suitable geosynthetics for use in new reinforced PMA pavement.

Table 4.1 Fabric effectiveness factor (FEF) of new reinforced polymer modified asphalt pavement

Type of Geosynthetics	FEF
Geogrid (NPGG)	1.38
Geocomposite (NPGT)	2.79
Geogrid+Geocomposite (NPGGGT)	1.15

4.4 Overlayed Unreinforced and Overlayed Reinforced Polymer Modified Asphalt Pavement

4.4.1 Footing settlement and Footing Permanent Settlement

Figure 4.11(a) compares the relationship between a footing pressure and the footing settlement in overlayed unreinforced and overlayed reinforced PMA pavement. Figure 4.11(b) compares the relationship between the footing settlement and the elapsed time in overlayed unreinforced and overlayed reinforced PMA pavement. Figure 4.11(c) compares a relationship between the permanent settlement of footing and the number of cycles of cyclic loading in overlayed unreinforced and overlayed reinforced PMA pavement. The following trends of behavior may be seen from Figure 4.11(a)-Figure 4.11(c):

1) Both the footing settlement and the footing permanent settlement were increased with an increase in the number of cycle of cyclic loading, the footing pressure and the elapsed time.
2) The footing settlement and the permanent settlement of the footing significantly decreased when with reinforced PMA pavement with geosynthetics, except reinforced with geogrid together with geocomposite. The overlayed PMA pavement reinforced with geogrid together with geocomposite (DMGGGT) showed a greater permanent settlement of the footing. The overlayed unreinforced PMA pavement (DMNO), overlayed PMA pavement reinforced with geocomposite (DMGT) and overlayed PMA pavement reinforced with geogrid (DMGG) exhibited footing settlement from a lower to a higher value, respectively. Reinforcing in overlayed pavement with geosynthetics can widely distribute pressure underneath model footing to a much wider area beneath, like new PMA pavement. Thus, the rigidity of pavement was increased and footing settlement and the permanent settlement of the footing decreased.
3) The rate of footing permanent settlement development decreased with an increase in the number of cycle of cyclic loading. That is, the footing permanent settlement relatively larger occurred in the first section of loading (approximate $N_c = 1$ to $N_c = 50$).Therfore, plastic deformations (irreversible deformation) occurred in some area of pavement underneath model footing. After that, the footing permanent settlement was less developed and was stable in the last section of loading. Due to occurrence of plastic deformation in the first section of loading, the plastic deformation was less distributed to new area of pavement.

4) The rate of footing permanent settlement development decreased when reinforced pavement with geosynthetics. This rate was calculated from occurrence of permanent deformation in the last section of loading because the permanent settlement of footing was less occurred and was rather stable. The footing permanent settlement rate in overlayed PMA pavement reinforced with geogrid (DMGG) was the less value for overlayed pavement that was equal to 0.00703 mm/cycle. The overlayed PMA pavement reinforced with geocomposite (DMGT), overlayed PMA pavement with reinforced geogrid together with geocomposite (DMGGGT) and overlayed unreinforced PMA pavement (DMNO) showed greater rates of footing permanent settlements that were equal to 0.01342, 0.01758 and 0.0177 mm/cycle, respectively.
5) From the above, the overlayed PMA pavement reinforced with geogrid (DMGG) was the most effective for resisting footing settlement and permanent settlement of the footing. From the determination of the covering ratio of geosynthetics (Equation 4.3), geogrid has a less covering ratio value, approximate equal to 25%. The contact area between new PMA pavement and old asphaltic concrete (HMA) pavement was the greatest in overlayed reinforced PMA pavement (75%). Thus, geogrid can be tightly integrated with new PMA pavement and old HMA pavement. The footing settlement and permanent settlement of the footing was also less.
6) From the above, the overlayed PMA pavement reinforced with geogrid together with geocomposite (DMGGGT) showed a greater footing settlement and permanent settlement of the footing. This situation may be due to slippage between reinforcements themselve. The geogrid and geocomposite were moved away from each other. Therefore, the performance of reinforcing effect was decreased.

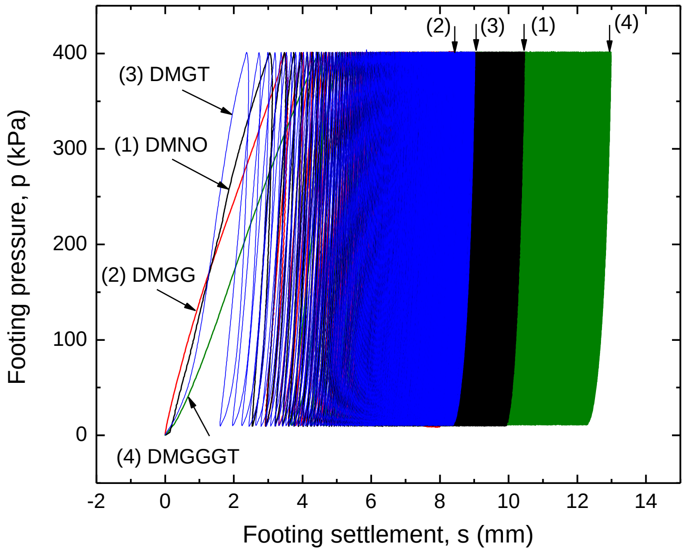

Figure 4.11(a) Relationship between footing pressure and footing settlement in overlayed unreinforced and overlayed reinforced polymer modified asphalt pavements

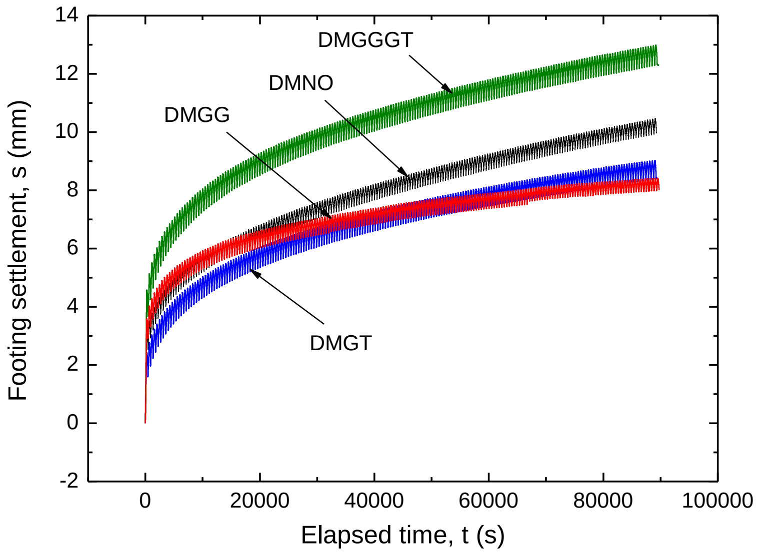

Figure 4.11(b) Relationship between footing settlement and elapsed time in overlayed unreinforced and overlayed reinforced polymer modified asphalt pavements

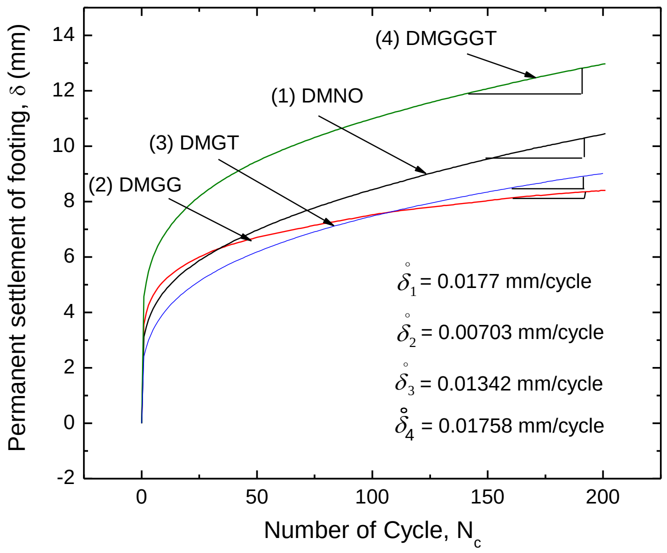

Figure 4.11(c) Relationship between permanent settlement of footing settlement and number of cycle in overlayed unreinforced and overlayed reinforced polymer modified asphalt pavements

4.4.2 Surface Settlement and Settlement Underneath Pavement

Figure 4.12(a) compares the relationship between the surface settlement and the distance from center of footing at different numbers of cycle for overlayed unreinforced and overlayed reinforced PMA pavement. Figure 4.12(b) compares the settlement underneath polymer modified asphalt pavement at different numbers of cycle for overlayed unreinforced and overlayed reinforced PMA pavement. The following trends of behavior may be seen from Figure 4.12(a) and Figure 4.12(b):

1) Both the surface settlement and the settlement underneath polymer modified asphalt pavement increased with an increase in the number of cycle of cyclic loading.
2) On the other hand, both the surface settlement and the settlement underneath polymer modified asphalt pavement decreased with an increase in the distance from center of footing.
3) The surface settlement significantly decreased when reinforced PMA pavement with geosynthetics, except reinforced with geogrid together with geocomposite. The overlayed PMA pavement reinforced with geogrid together with geocomposite (DMGGGT) showed the greatest surface settlement. The overlayed unreinforced PMA pavement (DMNO), overlayed PMA pavement reinforced with geocomposite (DMGT) and overlayed PMA pavement reinforced with geogrid (DMGG) exhibited surface settlement from a larger to a lower value, respectively.
4) The settlement underneath pavement significantly decreased with pavement reinforced with geosynthetics, except reinforced with geogrid together with geocomposite. The sequences of settlement were similar to those of surface settlement.
5) The trends of surface settlement and settlement underneath pavement were similar for both overlayed unreinforced and reinforced PMA pavement in the first section of loading ($N_c = 5$ and $N_c = 10$) and the last section of loading ($N_c = 190$, $N_c = 195$ and $N_c = 200$). The direction of surface settlement and settlement underneath pavement were downward at center of footing and 60 mm from center of footing; but, these directions were upward at approximately 100 mm from center of footing.
6) From the above, reinforcing in overlayed PMA pavement with geosynthetics can improve rigidity of pavement, especially reinforcing with geogrid. Thus, rutting, a distress type in pavement, was possibly decreased when reinforcing overlayed PMA pavement with geosynthetics.

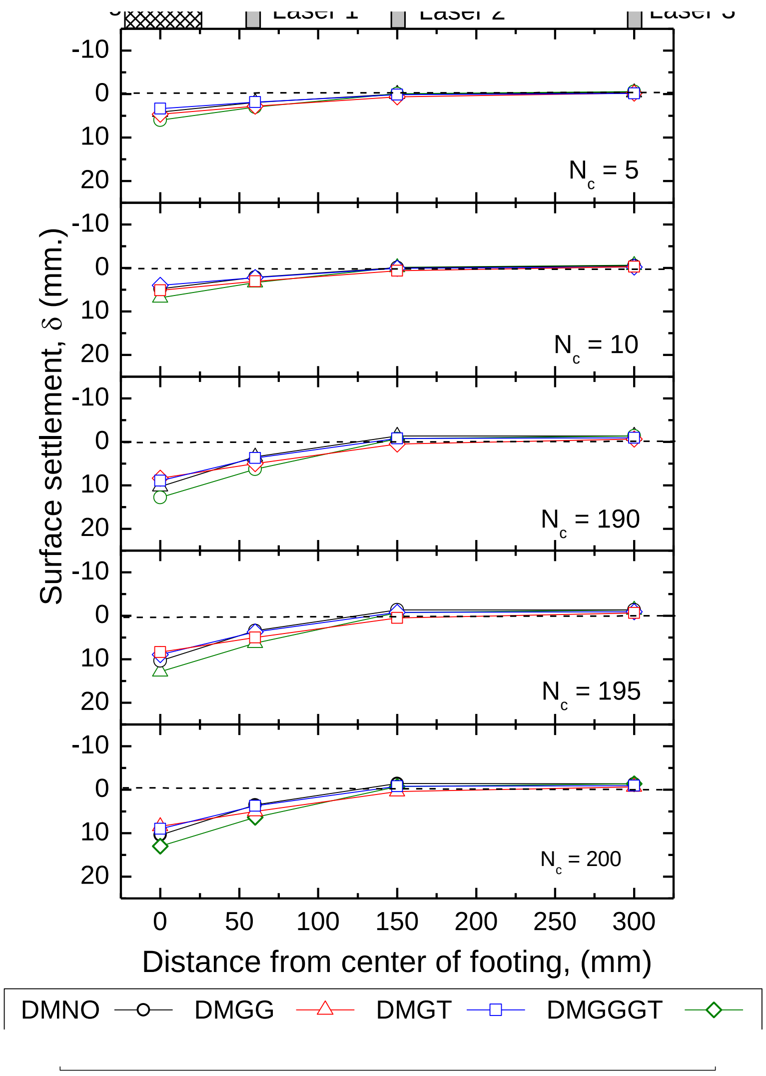

Figure 4.12(a) Relationship between surface settlement and distance from center of footing in overlayed unreinforced and overlayed reinforced polymer modified asphalt pavements

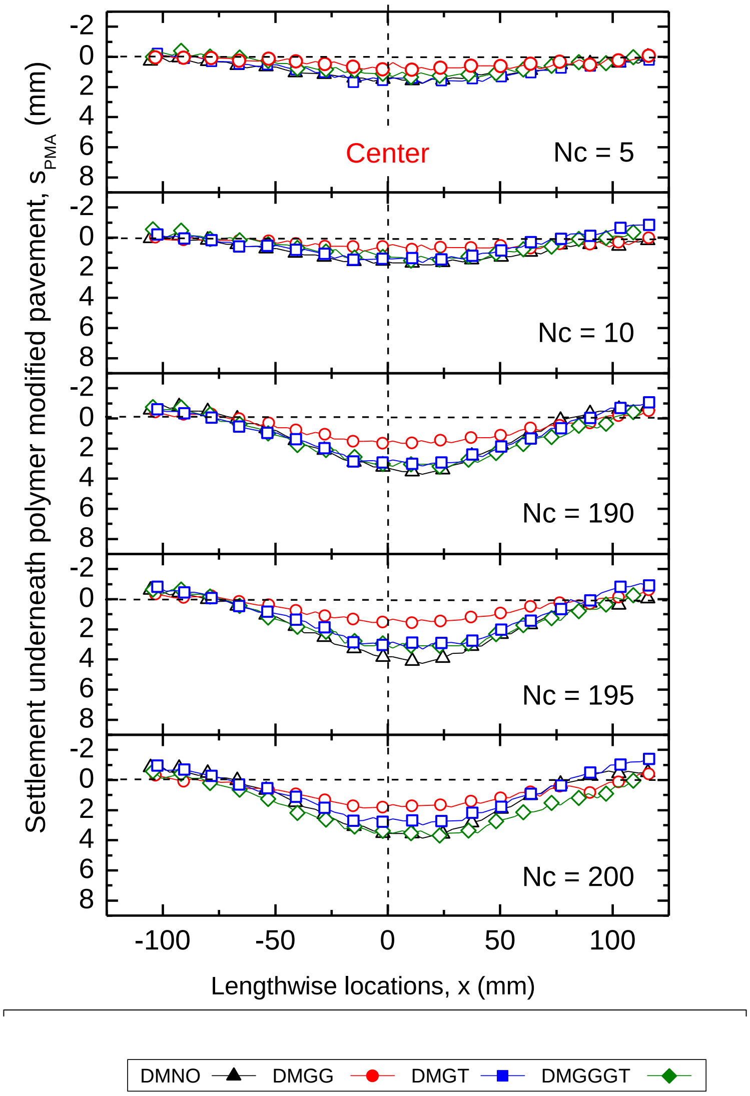

Figure 4.12(b) Settlement underneath polymer modified asphalt pavement in overlayed unreinforced and overlayed reinforced polymer modified asphalt pavements

4.4.3 Strain Field of Sand Subbase

Figure 4.13(a) shows maximum shear strain ($\gamma_{\max}$) distribution in overlayed unreinforced PMA pavement at 200 cycles of cyclic loading. Figure 4.13(b) shows maximum shear strain ($\gamma_{\max}$) distribution in overlayed PMA pavement reinforced with geogrid at 200 cycles of cyclic loading. Figure 4.13(c) shows maximum shear strain ($\gamma_{\max}$) distribution in overlayed PMA pavement reinforced with geocomposite at 200 cycles of cyclic loading. Figure 4.13(d) shows maximum shear strain ($\gamma_{\max}$) distribution in overlayed PMA pavement reinforced with geogrid together with geocomposite at 200 cycles of cyclic loading. Figure 4.13(e) shows relationship between average of $\gamma_{\max}$ and number of cycle in overlayed unreinforced and overlayed reinforced polymer modified asphalt pavements. The following trends of behavior may be seen from Figure 4.13(a)-Figure 4.13(e):

1) The maximum shear strain ($\gamma_{\max}$) distribution was significantly decreased for pavement reinforced with geosynthetics, except reinforced with geogrid together with geocomposite. The overlayed unreinforced PMA pavement (DMNO) and overlayed PMA pavement reinforced with geogrid together with geocomposite (DMGGGT) showed a greater maximum shear strain ($\gamma_{\max}$) distribution under the modelfooting. The overlayed PMA pavement reinforced with geogrid (DMGG) and overlayed PMA pavement reinforced with geocomposite (DMGT) showed a less and lesser maximum shear strain ($\gamma_{\max}$) distribution, respectively.
2) A shear band may occurred along maximum shear strain ($\gamma_{\max}$) distribution direction under footing in overlayed unreinforced PMA pavement (DMNO) and overlayed PMA pavement reinforced with geogrid together with geocomposite (DMGGGT). Therefore, subbase failure may occurred along direction of shear band in these two cases before other two cases (the overlayed PMA pavement reinforced with geogrid (DMGG) and overlayed PMA pavement reinforced with geocomposite (DMGT)).
3) The rate of maximum shear strain ($\gamma_{\max}$) development significantly decreased when reinforced PMA pavement with geosynthetics. The overlayed unreinforced PMA pavement (DMNO) showed the greatest rate of maximum shear strain ($\gamma_{\max}$) development among overlayed PMA pavements, equal to 0.02953 %/cycle. The overlayed PMA pavement reinforced with geocomposite (DMGT), overlayed PMA pavement reinforced with geogrid together with geocomposite (NPGGGT) and overlayed reinforced PMA pavement with geogrid (NPGG) exhibited the rate of maximum shear strain ($\gamma_{\max}$) development from a greater to lower values that were equal to 0.02875, 0.02792 and 0.0232 %/cycle, respectively. Therefore, the maximum shear strain ($\gamma_{\max}$) may be the less occurred in overlayed PMA reinforced pavement with geogrid (DMGG) among overlayed PMA pavements.
4) From the above, the use of geosynthetic reinforcement for reinforcing of overlayed PMA pavement can widely distribute pressure underneath model footing to a wider area underneath.

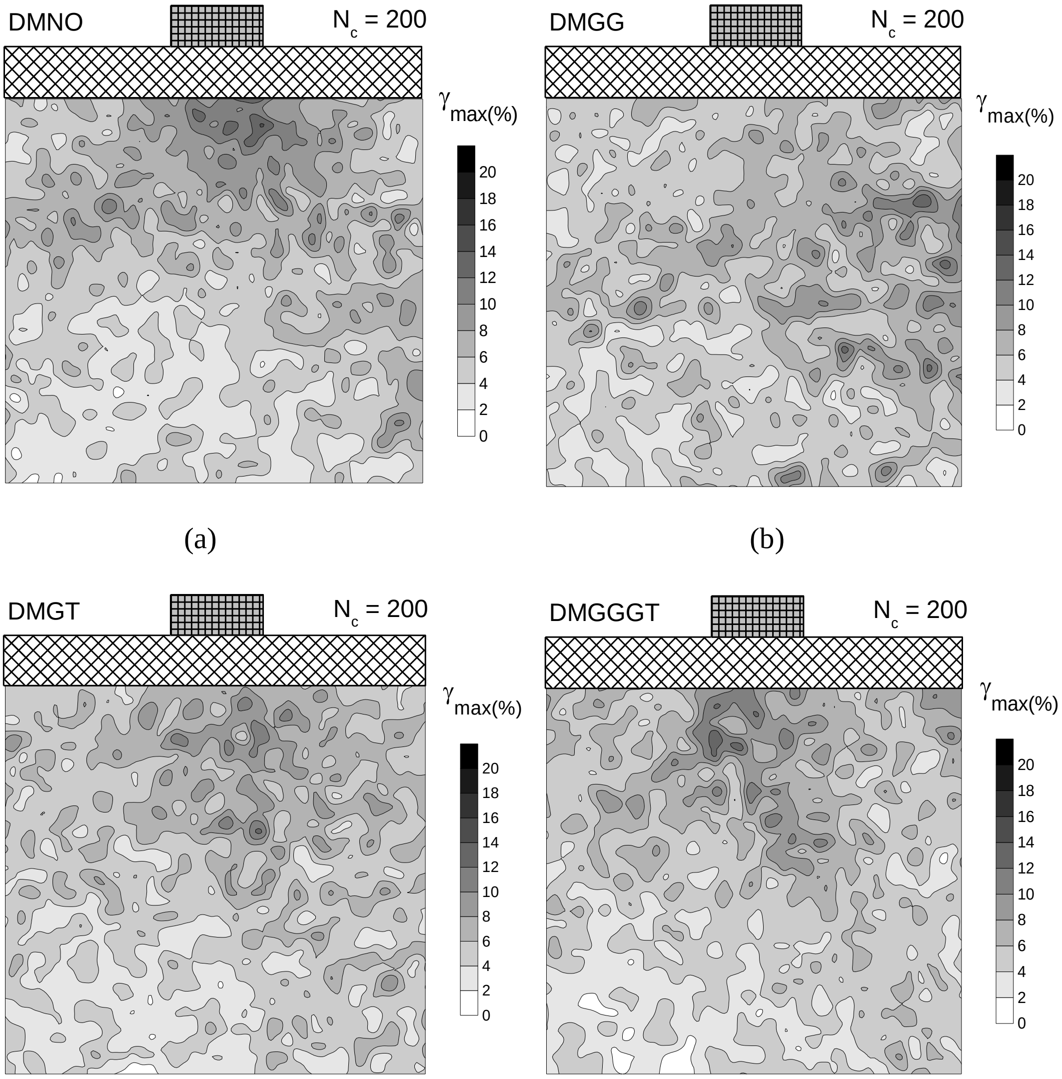

(a) (b)

(c) (d)

Figure 4.13 Maximum shear strain distribution at 200 cycles of cyclic loading; (a) overlayed unreinforced PMA pavement (DMNO), (b) overlayed PMA pavement reinforced with geogrid (DMGG), (c) overlayed PMA pavement reinforced with geocomposite (DMGT) and (d) overlayed PMA pavement reinforced with geogrid together with geocomposite (DMGGGT)

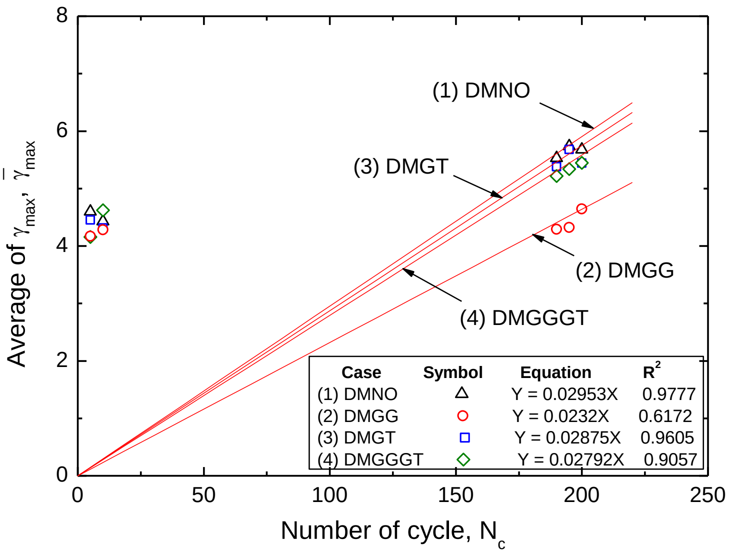

Figure 4.13(e) Relationship between average of γ_{max} and number of cycle in overlayed unreinforced and overlayed reinforced polymer modified asphalt pavements

4.4.4 Surface Cracking

Figure 4.14(a) shows surface cracking in overlayed unreinforced PMA pavement (DMNO). Figure 4.14(b) shows surface cracking in overlayed PMA pavement reinforced with geogrid (DMGG). Figure 4.14(c) shows surface cracking in overlayed PMA pavement reinforced with geocomposite (DMGT). Figure 4.14(d) shows surface cracking in overlayed PMA pavement reinforced with geogrid together with geocomposite (DMGGGT)

From Figure 4.14(a), surface cracking in overlayed unreinforced pavement could not be observed, because pavement was broken while moving out from the container.

From Figure 4.14(b) to Figure 4.14(d), the surface cracking in overlayed PMA pavement reinforced with geogrid together with geocomposite (DMGGGT) was the greatest seen among overlayed PMA pavements. And, the surface cracking in overlayed PMA pavement reinforced with geogrid (DMGG) was the smallest seen among overlayed PMA pavements. The surface crackings were exhibited around the edge og model footing (dash rectangular line). Therefore, reinforcing with geogrid in overlayed PMA pavement was the best in decreasing the surface cracking around area that wheel was contacted onto pavement in this study.

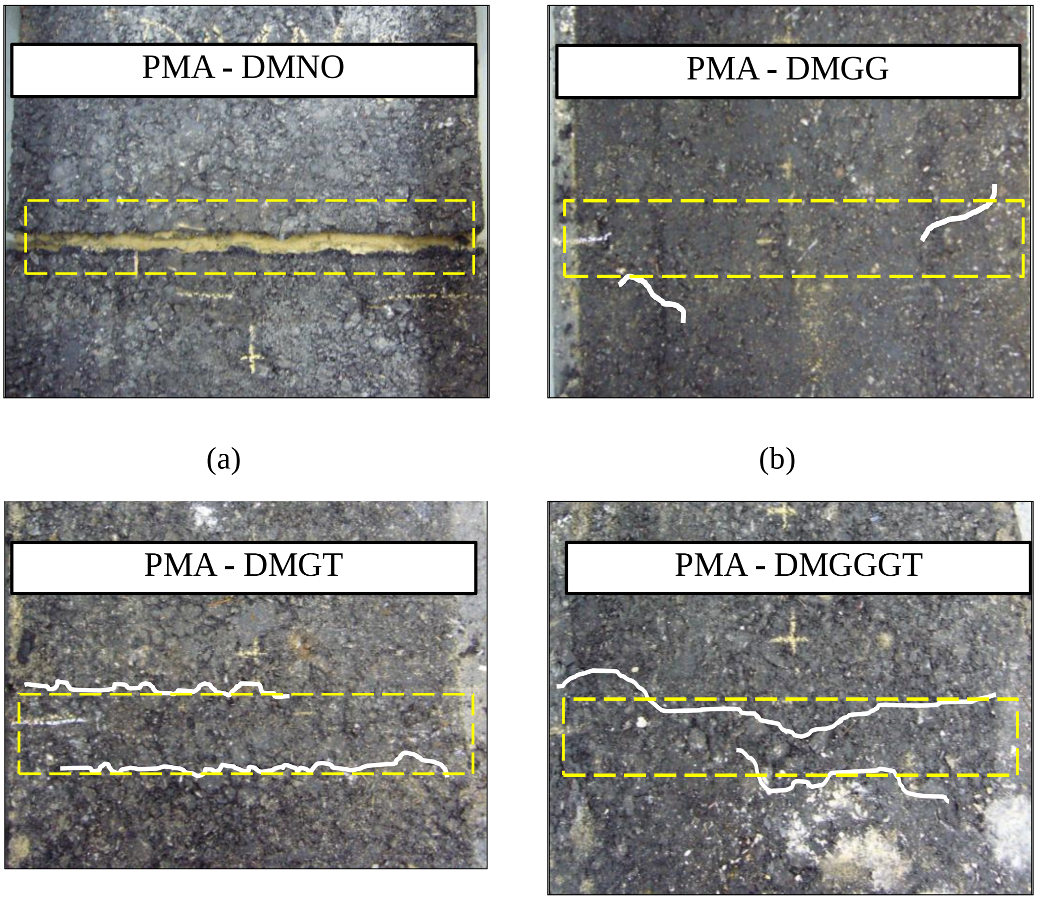

(a) (b)

(c) (d)

Figure 4.14 Surface cracking in polymer modified asphalt pavements; (a) overlayed unreinforced PMA pavement (DMNO), (b) overlayed PMA pavement reinforced with geogrid (DMGG), (c) overlayed PMA pavement reinforced with geocomposite (DMGT) and (d) overlayed PMA pavement reinforced with geogrid together with geocomposite (DMGGGT)

4.4.5 Fabric Effective Factor

From Table 4.2, FEF value in overlayed PMA pavement reinforced with geogrid (DMGG) showed a greatest value among overlayed pavements, equal to 1.24. The overlayed PMA pavement reinforced with geocomposite (DMGT) and overlayed PMA pavement reinforced with geogrid together with geocomposite (DMGGGT) showed a less FEF value, equal to 1.16 and 0.81, respectively. When comparing the performance of overlayed reinforced PMA pavement, the pavement reinforced with geogrid (DMGG) was the most effective for this study. Thus, geogrid was a suitable geosynthetics for use in overlayed reinforced PMA pavement. On the other hand, the pavement reinforced with geogrid together with geocomposite (DMGGGT) was not effective for of improvement the performance of overlayed PMA pavement.

Table 4.2 Fabric effectiveness factor (FEF) of overlayed reinforced polymer modified asphalt pavement

Type of Geosynthetics	FEF
Geogrid (DMGG)	1.24
Geocomposite (DMGT)	1.16
Geogrid+Geocomposite (DMGGGT)	0.81

4.5 Comparison of Polymer Modified Asphalt (PMA) and Asphaltic Concrete (HMA) Pavement among New Pavement Cases

All of the test results of asphaltic concrete (HMA) pavement were referred to Thaisri (2009).

4.5.1 Footing settlement and Footing Permanent Settlement

Figure 4.15(a) compares the relationship between the footing pressure and the footing settlement for new unreinforced PMA and HMA pavements. Figure 4.15(b) compares the relationship between the footing pressure and the footing settlement for new PMA and HMA pavements reinforced with geogrid. Figure 4.15(c) compares the relationship between the footing pressure and a footing settlement for new PMA and HMA pavements reinforced with geocomposite.

Figure 4.16(a) compares the relationship between the footing settlement and the elapsed time for new unreinforced PMA and HMA pavements. Figure 4.16(b) compares the relationship between the footing settlement and the elapsed time for new PMA and HMA pavements reinforced with geogrid. Figure 4.16(c) compares the relationship between the footing settlement and the elapsed time for new PMA and HMA pavements reinforced with geocomposite.

Figure 4.17(a) compares the relationship between the permanent settlement of footing and the number of cycles of cyclic loading for new unreinforced PMA and HMA pavements. Figure 4.17(b) compares the relationship between the permanent settlement of footing and the number of cycles of cyclic loading for new PMA and HMA pavements reinforced with geogrid and Figure 4.17(c) compares the relationship between the permanent settlement of footing and the number of cycles of cyclic loading in new PMA and HMA pavements reinforced with geocomposite.

Table 4.3 shows the ratio of permanent settlement of footing between new PMA and HMA pavement at number of cycle of 200.

The following trends of behavior may be seen from Figure 4.15-Figure 4.17 and Table 4.3:

1) Both the footing settlement and the footing permanent settlement increased with an increase in the number of cycle of cyclic loading, the footing pressure and the elapsed time.

2) The footing settlement and the permanent settlement of the footing significantly decreased by using PMA for pavement, as shown in following details:

   a) For new unreinforced PMA and HMA pavements, new unreinforced HMA pavement showed a greater footing settlement and the permanent settlement of the footing at the same time.

   b) For new PMA and HMA pavements reinforced with geogrid, new HMA pavement reinforced with geogrid showed a greater footing settlement and the permanent settlement of the footing at the same time.

   c) For new PMA and HMA pavements reinforced with geocomposite, new HMA pavement reinforced with geocomposite showed a greater footing settlement and the permanent settlement of the footing at the same time.

3) When comparing the permanent settlement of footing at 200 cycles of cyclic loading between new PMA and HMA pavements, the ratio of new unreinforced, reinforced with geogrid and reinforced with geocomposite were equal to 1.22, 1.55 and 2.06, respectively. Thus, the new PMA pavements were more effective in resisting permanent settlement of footing than the new HMA pavements.

4.) The rate of footing permanent settlement development was decreased with an increase in the number of cycle of cyclic loading. That is, the footing permanent settlement relative largely occurred in the first section of loading (approximate $N_c = 1$ to $N_c = 50$). Then, plastic deformation (irreversible deformation) occurred in some area of pavement structure underneath the model footing. After that, the footing permanent settlement became less occurred and stable in the last section of loading. Due to occurrence of plastic deformation in the first section of loading, the plastic deformation was less distributed to new area of pavement.

5.) From the above, replacing asphalt cement (AC) with polymer modified asphalt cement (PM-AC) increased stiffness (hardness) of pavement. Therefore, PMA pavement may be less sensitive to permanent deformation. It was possibly considered that polymer addition in asphalt cement minimized the pavement deficiencies revealed due to aging and can provide an increase in the service life of the road.

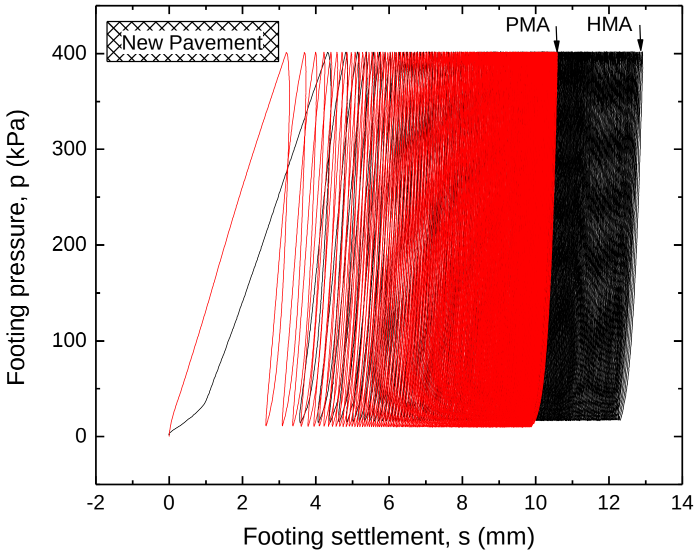

Figure 4.15(a) Relationship between footing pressure and footing settlement in new unreinforced PMA and HMA pavements

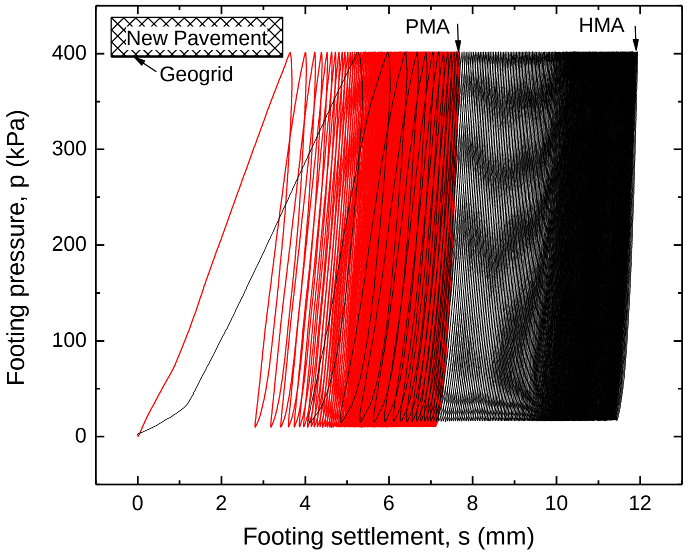

Figure 4.15(b) Relationship between footing pressure and footing settlement in new PMA and HMA pavements reinforced with geogrid

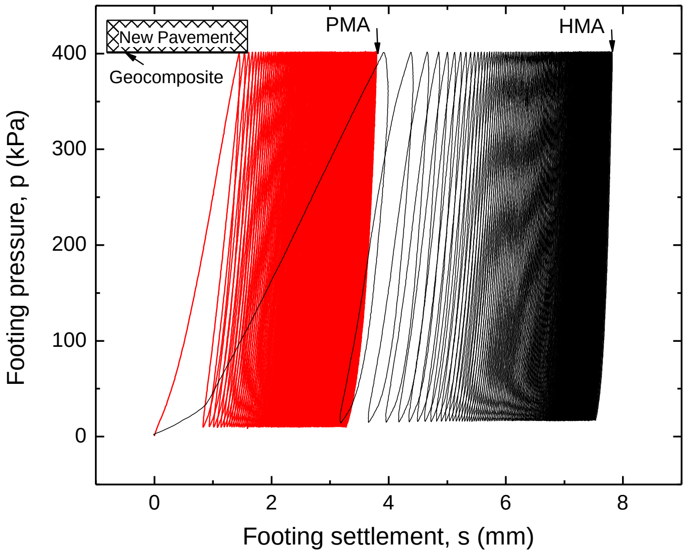

Figure 4.15(c) Relationship between footing pressure and footing settlement in new PMA and HMA pavements reinforced with geocomposite

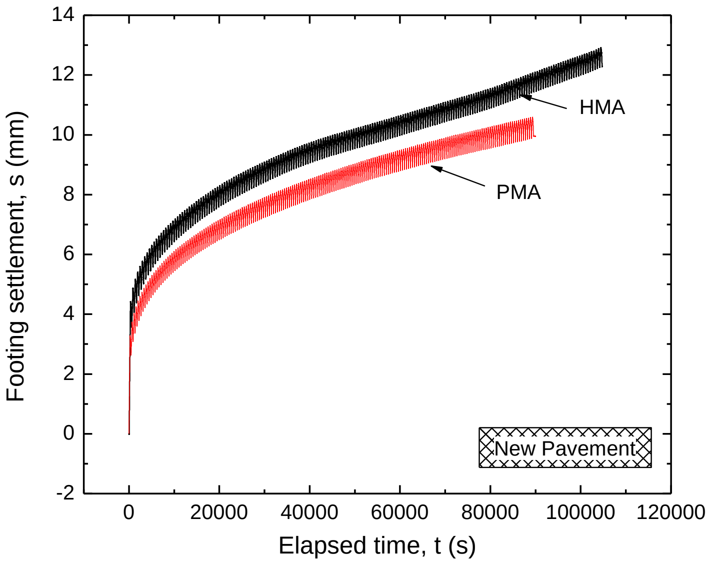

Figure 4.16(a) Relationship between footing settlement and elapsed time in new unreinforced PMA and HMA pavements

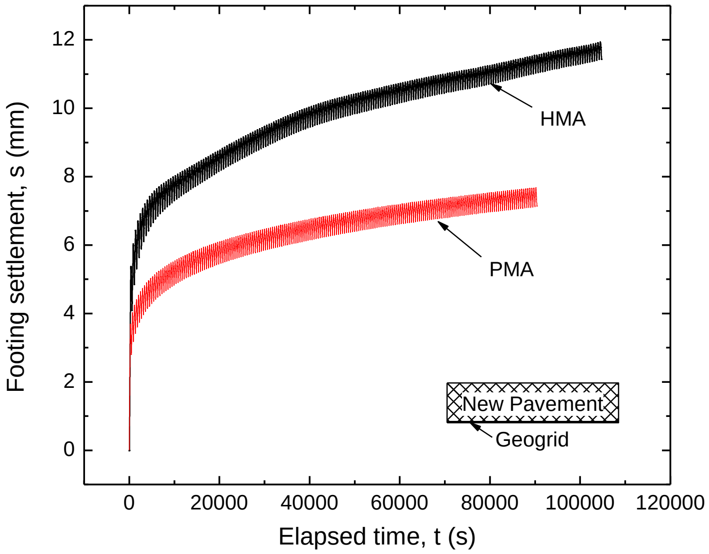

Figure 4.16(b) Relationship between footing settlement and elapsed time in new PMA and HMA pavements reinforced with geogrid

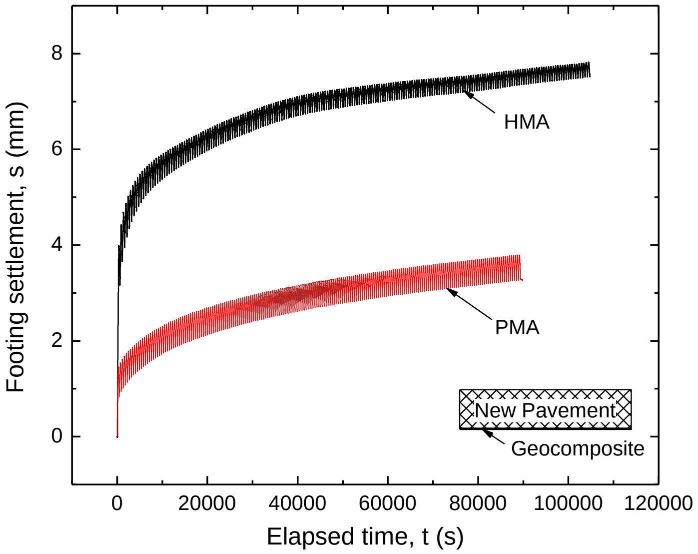

Figure 4.16(c) Relationship between footing settlement and elapsed time in new PMA and HMA pavements reinforced with geocomposite

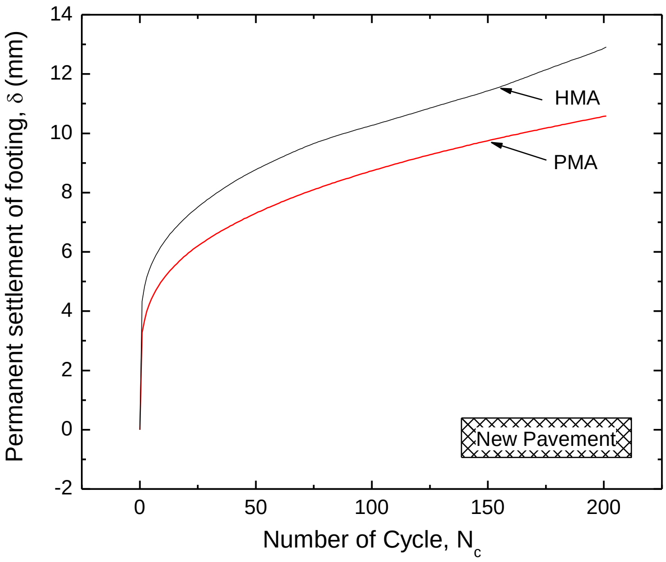

Figure 4.17(a) Relationship between permanent settlement of footing and number of cycle in new unreinforced PMA and HMA pavements

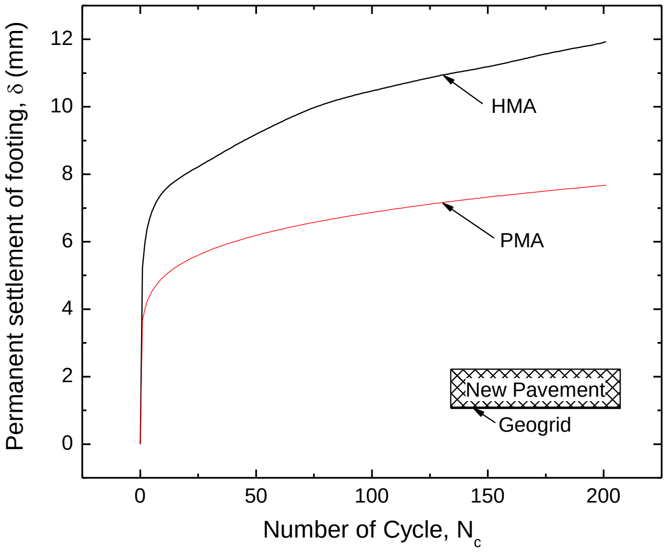

Figure 4.17(b) Relationship between permanent settlement of footing and number of cycle in new PMA and HMA pavements reinforced with geogrid

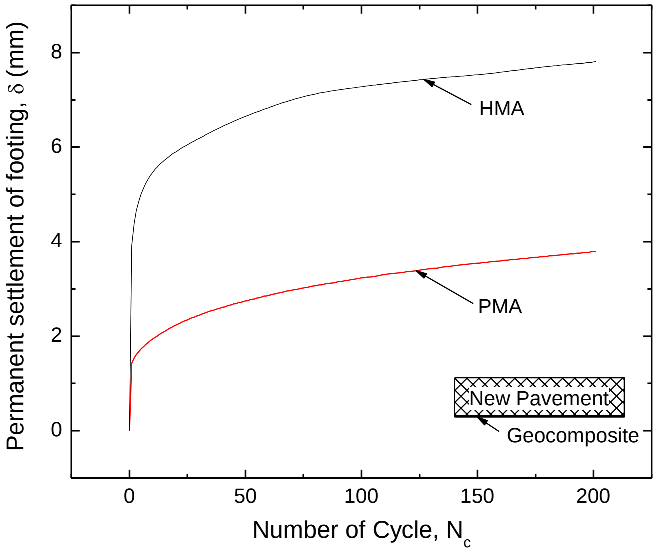

Figure 4.17(c) Relationship between permanent settlement of footing and number of cycle in new PMA and HMA pavements reinforced with geocomposite

Table 4.3 Ratio of permanent settlement of footing between new PMA and HMA pavement at 200 cycles of cyclic loading

Type of Reinforcement	**Ratio of permanent settlement of footing between new PMA and HMA pavement** $(\frac{\delta_{HMA}}{\delta_{PMA}})$ **at 200 cycles of cyclic loading**
Unreinforced (NPNO)	1.22
Reinforced with geogrid (NPGG)	1.55
Reinforced with geocomposite (NPGT)	2.06

4.5.2 Surface Settlement and Settlement Underneath Pavement

Figure 4.18(a) compares the relationship between the surface settlement and the distance from center of footing for different numbers of cycles for new unreinforced PMA and HMA pavement. Figure 4.18(b) compares the relationship between the surface settlement and the distance from center of footing for different numbers of cycle for new PMA and HMA pavements reinforced with geogrid. Figure 4.18(c) compares the relationship between the surface settlement and the distance from center of footing for different number of cycles for new PMA and HMA pavements reinforced with geocomposite.

Figure 4.19(a) compares the settlement underneath asphalt pavement for different number of cycle for new unreinforced PMA and HMA pavements. Figure 4.19(b) compares a settlement underneath asphalt pavement for different number of cycle for new PMA and HMA pavements reinforced with geogrid and Figure 4.19(b) compares a settlement underneath asphalt pavement for different number of cycle for new PMA and HMA pavements reinforced with geocomposite.

The following trends of behavior may be seen from Figure 4.18 and Figure 4.19:

1) Both the surface settlement and the settlement underneath asphalt pavement increased with an increase in the number of cycle of cyclic loading.
2) On the other hand, both the surface settlement and the settlement underneath asphalt pavement decreased with an increase in the distance from center of footing.
3) The surface settlement and settlement underneath pavement significantly decreased in PMA pavement, as shown in following details:
   a) For new unreinforced PMA and HMA pavement, new unreinforced HMA pavement showed a greater footing surface settlement and settlement underneath pavement at the same cycle of cyclic loading.
   b) For new PMA and HMA pavements reinforced with geogrid, new HMA pavement reinforced with geogrid showed a greater footing surface settlement and settlement underneath pavement at the same cycle of cyclic loading.
   c) For new PMA and HMA pavements reinforced with geocomposite, new HMA pavement reinforced with geocomposite showed a greater footing surface settlement and settlement underneath pavement at the same cycle of cyclic loading.
4) The trend of surface settlement and settlement underneath pavement were different between PMA and HMA pavements in the first section of loading (N_c = 5 and N_c = 10) and the last section of loading (N_c = 190, N_c = 195 and N_c = 200). For new PMA pavements, the direction of surface settlement and settlement underneath pavement downward for all distance from center along the lengthwise direction. On the other hand, the direction of surface settlement and settlement underneath pavement were downward at center, but, it became upward at approximately 90 mm from center of footing in HMA pavements.
5) From the above, the new HMA pavements were susceptible to a large bending moment along the longwise direction of pavement. Thus, the resistance of surface settlement of PMA pavements was greater than the resistance of surface settlement of HMA pavements. The cracking in HMA pavements may be probably occurred easier than in PMA.

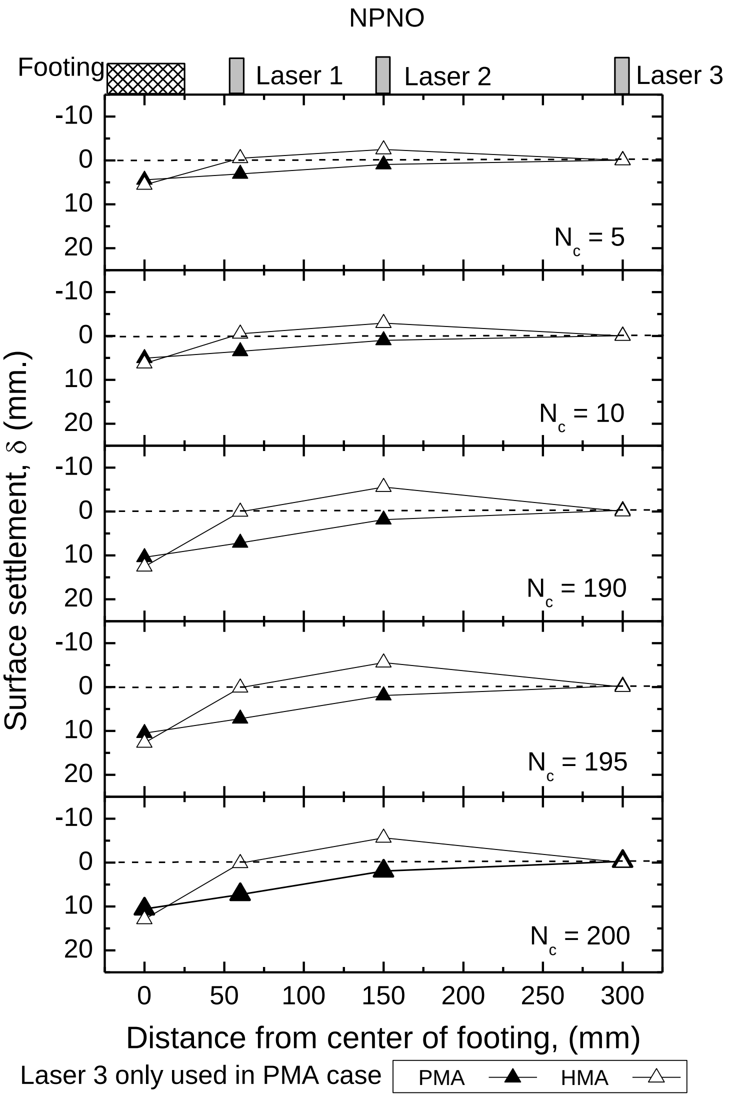

Figure 4.18(a) Relationship between surface settlement and distance from center of footing in new unreinforced PMA and HMA pavements

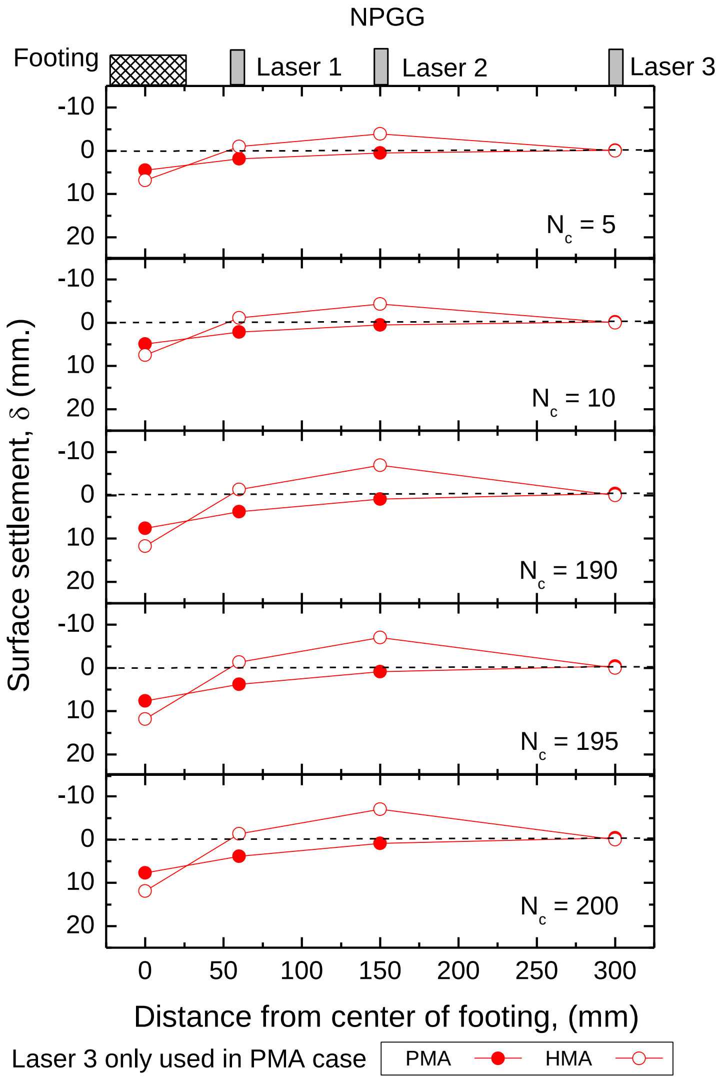

Figure 4.18(b) Relationship between surface settlement and distance from center of footing in new PMA and HMA pavements reinforced with geogrid

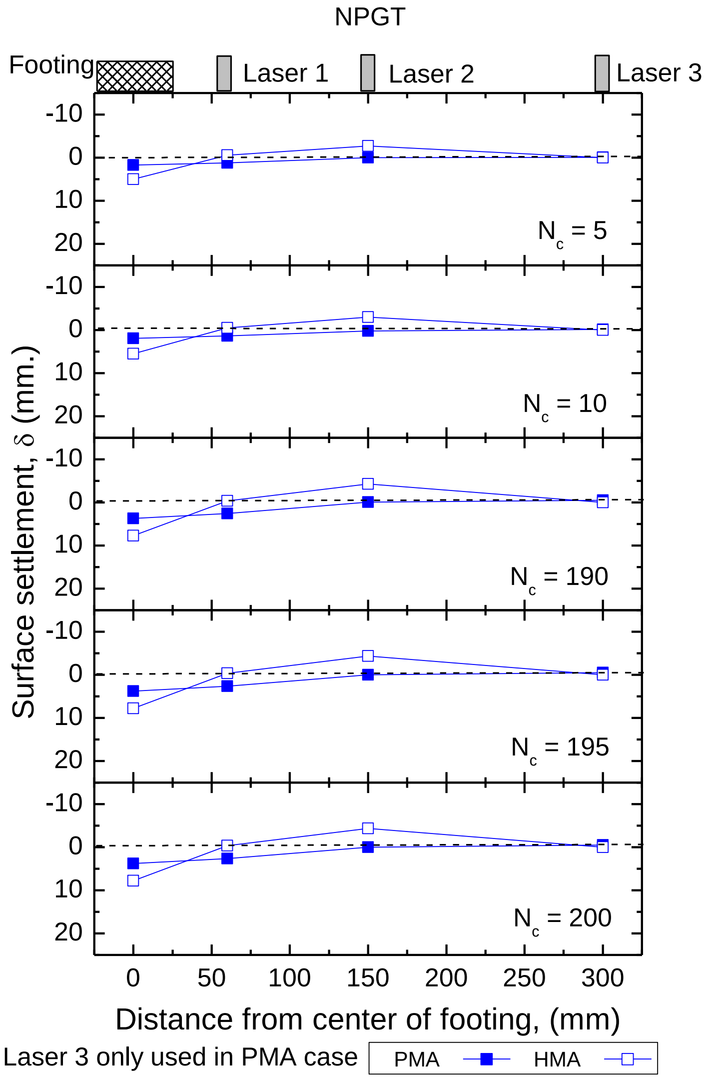

Figure 4.18(c) Relationship between surface settlement and distance from center of footing in new PMA and HMA pavements reinforced with geocomposite

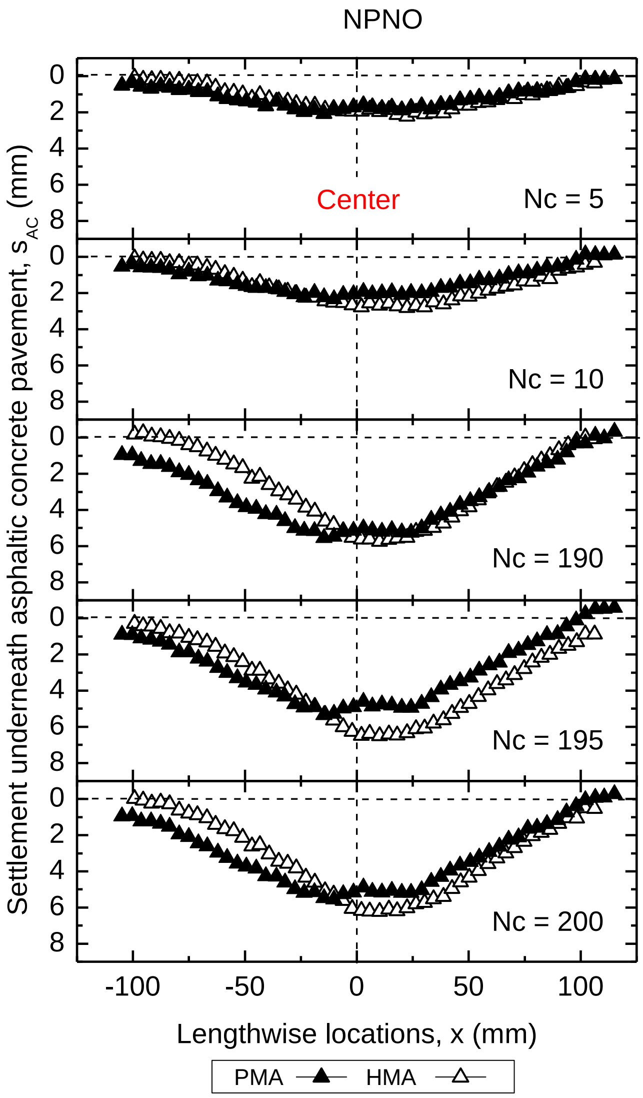

Figure 4.19(a) Settlement underneath asphalt pavement in new unreinforced PMA and HMA pavements

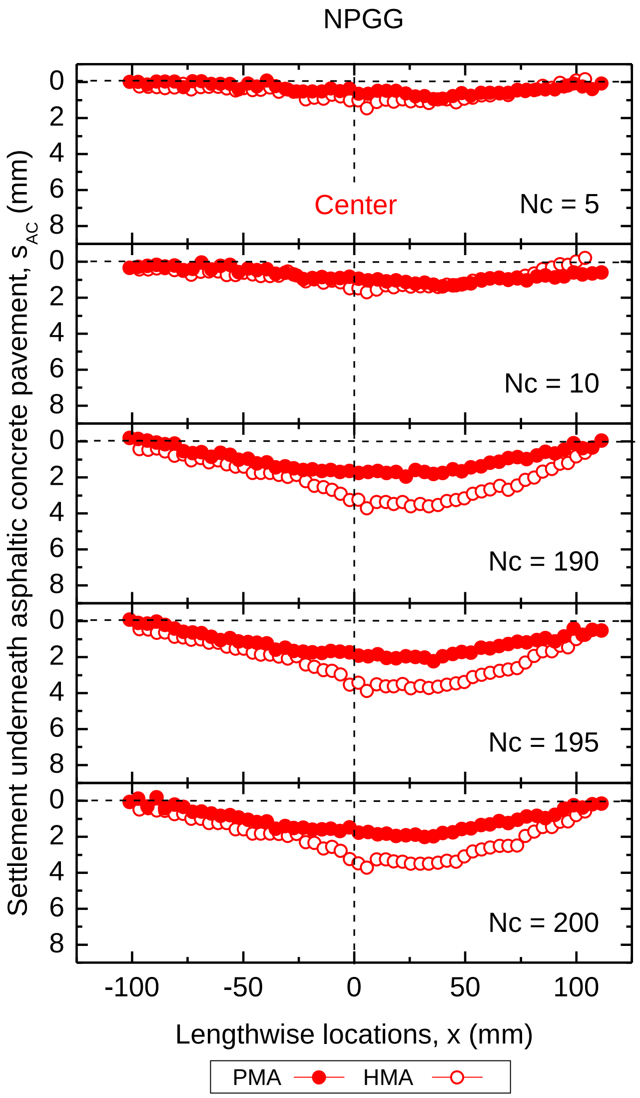

Figure 4.19(b) Settlement underneath asphalt pavement in new PMA and HMA pavements reinforced with geogrid

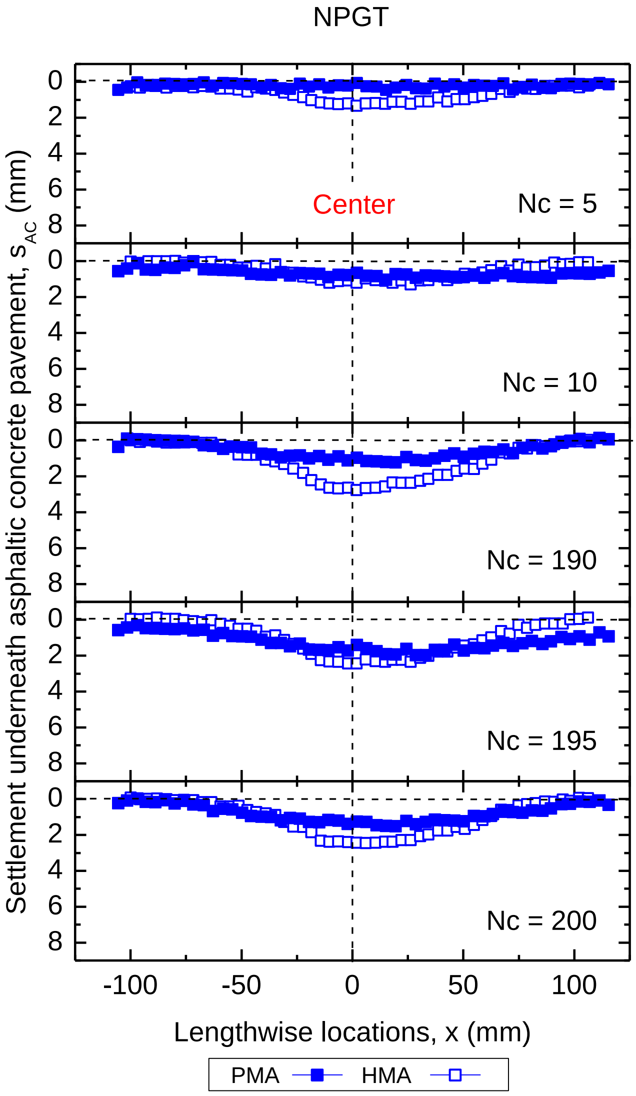

Figure 4.19(c) Settlement underneath asphalt pavement in new PMA and HMA pavements reinforced with geocomposite

4.5.3 Strain Field of Sand Subbase

Figure 4.20(a) shows maximum shear strain ($\gamma_{\max}$) distribution in new unreinforced PMA pavement at 200 cycles of cyclic loading. And, Figure 4.20(b) shows maximum shear strain ($\gamma_{\max}$) distribution in new unreinforced HMA pavement at 200 cycles of cyclic loading.

Figure 4.21(a) shows maximum shear strain ($\gamma_{\max}$) distribution in new PMA pavement reinforced with geogrid at 200 cycles of cyclic loading. And, Figure 4.21(b) shows maximum shear strain ($\gamma_{\max}$) distribution in new HMA pavement reinforced with geogrid at 200 cycles of cyclic loading.

Figure 4.22(a) shows maximum shear strain ($\gamma_{\max}$) distribution in new PMA pavement reinforced with geocomposite at 200 cycles of cyclic loading. And, Figure 4.22(b) shows maximum shear strain ($\gamma_{\max}$) distribution in new HMA pavement reinforced with geocomposite at 200 cycles of cyclic loading.

Figure 4.23(a) shows relationship between average of $\gamma_{\max}$ and number of cycle in new unreinforced PMA and HMA pavements. Figure 4.23(b) shows relationship between average of $\gamma_{\max}$ and number of cycle in new reinforced with geogrid PMA and HMA pavements. Figure 4.23(c) shows relationship between average of $\gamma_{\max}$ and number of cycle in new reinforced with geocomposite PMA and HMA pavements.

The following trends of behavior may be seen from Figure 4.20 to Figure 4.23:

1) The maximum shear strain ($\gamma_{\max}$) distribution significantly decreased with PMA pavement, as shown in following details:
   a) For new unreinforced PMA and HMA pavements, new unreinforced HMA pavement showed a greater maximum shear strain ($\gamma_{\max}$) distribution under footing. Also, the size of shear band in new unreinforced HMA pavement was larger than size of shear band in new unreinforced PMA pavement.
   b) For new reinforced with geogrid PMA and HMA pavements, new HMA pavement reinforced with geogrid showed a greater maximum shear strain ($\gamma_{\max}$) distribution. The shear band can be rather seen in new HMA pavement reinforced with geogrid. Thus, the shear band may occurred along maximum shear strain ($\gamma_{\max}$) distribution direction under footing in this pavement.
   c) For new PMA and HMA pavements reinforced with geocomposite, new HMA pavement reinforced with geocomposite showed a greater maximum shear strain ($\gamma_{\max}$) distribution.
2) The rate of maximum shear strain ($\gamma_{\max}$) development significantly decreased PMA pavement, as shown in following details:
   a) New unreinforced HMA pavement showed a greater rate of maximum shear strain ($\gamma_{\max}$) development, while new unreinforced PMA pavement showed a lower rate of maximum shear strain ($\gamma_{\max}$) development.

b) For new reinforced with geogrid PMA and HMA pavements, rate of maximum shear strain ($\gamma_{\max}$) development slightly differed between PMA pavement and HMA pavement.

c) For new PMA and HMA pavements reinforced with geocomposite, new PMA pavement reinforced with geocomposite showed a greater rate of maximum shear strain ($\gamma_{\max}$) development.

3) From the above, the appearance of shear band may be greater in new HMA pavements. The subbase failure may also be greater occurred along direction of shear band in new HMA pavements. Thus, the replacing asphalt cement (AC) with polymer modified asphalt cement (PM-AC), can reduce susceptibity of decreased failure in subbase pavement.

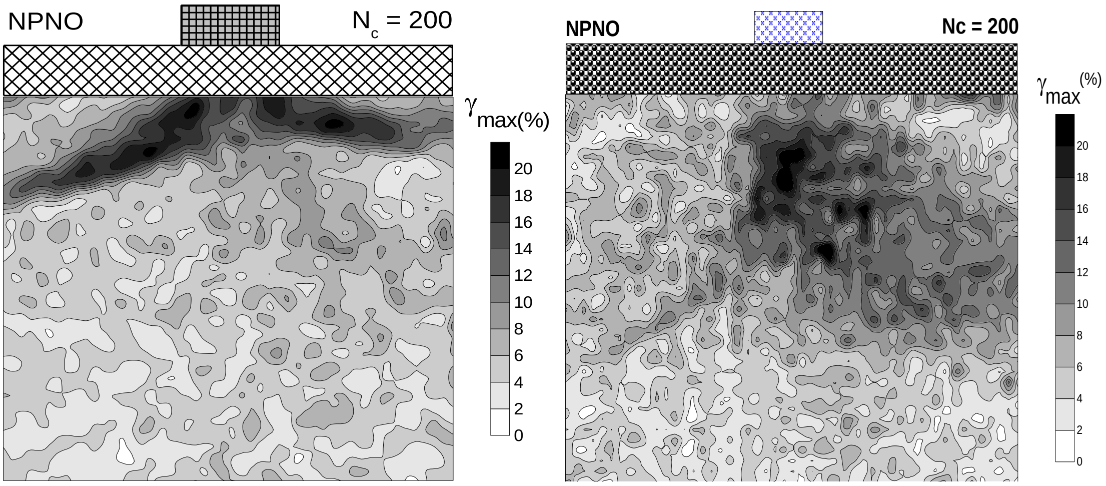

(a) (b)

Figure 4.20 Maximum shear strain distribution in new unreinforced pavements at 200 cycles of cyclic loading: (a) PMA pavement; and (b) HMA pavement

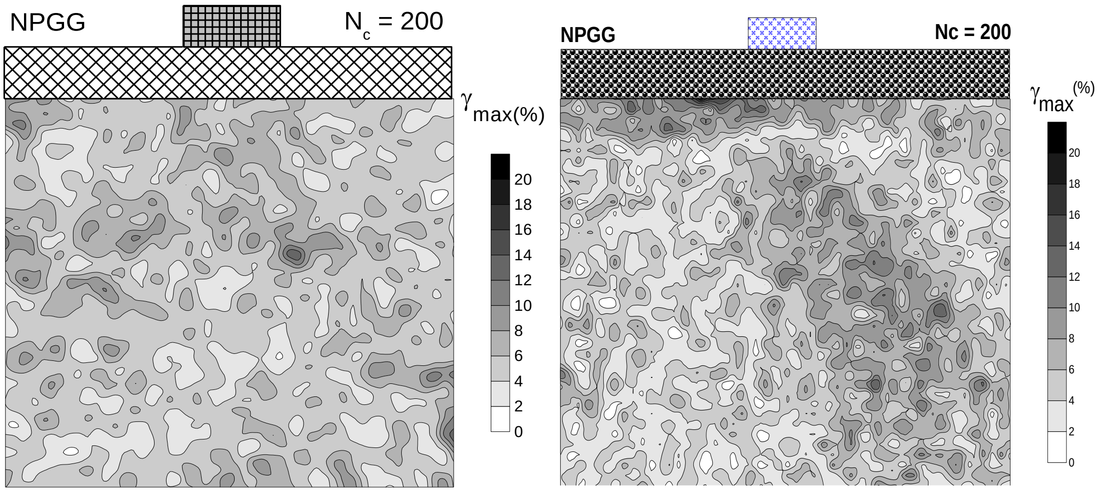

(a) (b)

Figure 4.21 Maximum shear strain distribution in new pavements reinforced with geogrid at 200 cycles of cyclic loading: (a) PMA pavement; and (b) HMA pavement

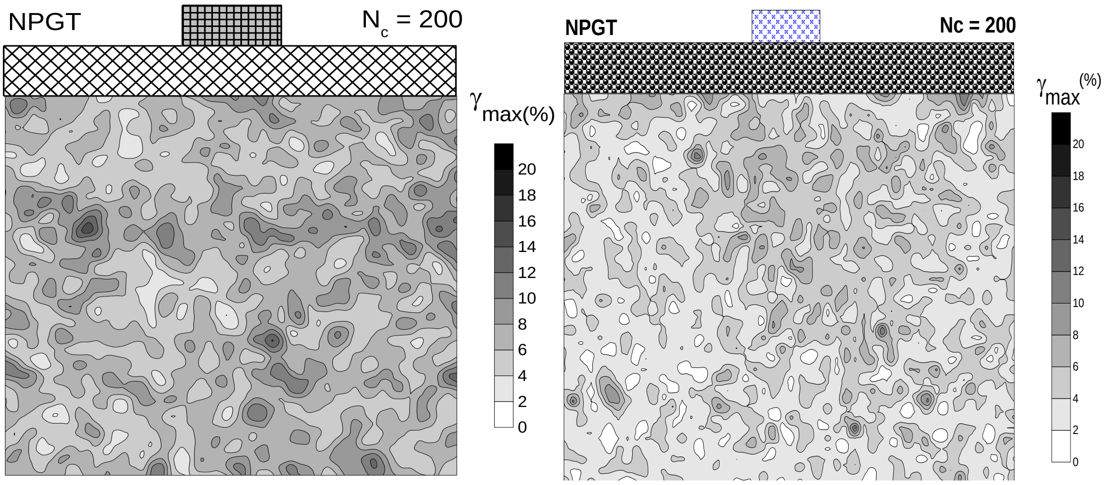

(a) (b)

Figure 4.22 Maximum shear strain distribution in new pavements reinforced with geocomposite at 200 cycles of cyclic loading: (a) PMA pavement; and (b) HMA pavement

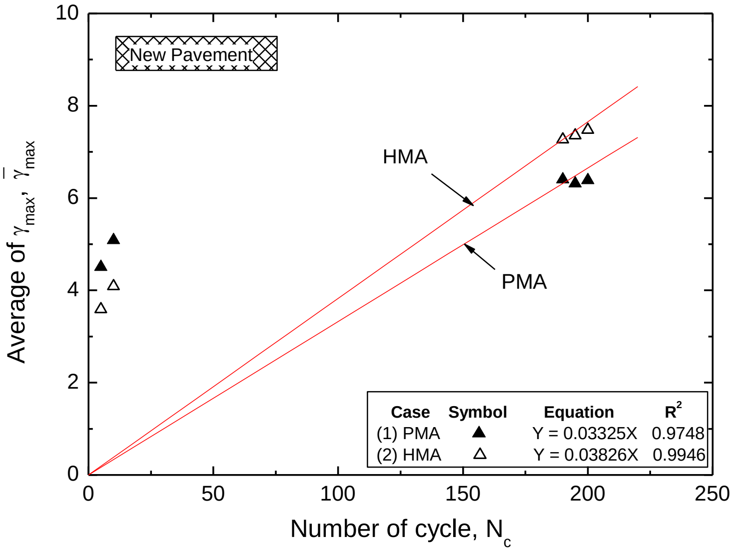

Case	Symbol	Equation	R^2
(1) PMA	▲	Y = 0.03325X	0.9748
(2) HMA	△	Y = 0.03826X	0.9946

Figure 4.23(a) Relationship between average of γ_{max} and number of cycle in new unreinforced PMA and HMA pavements

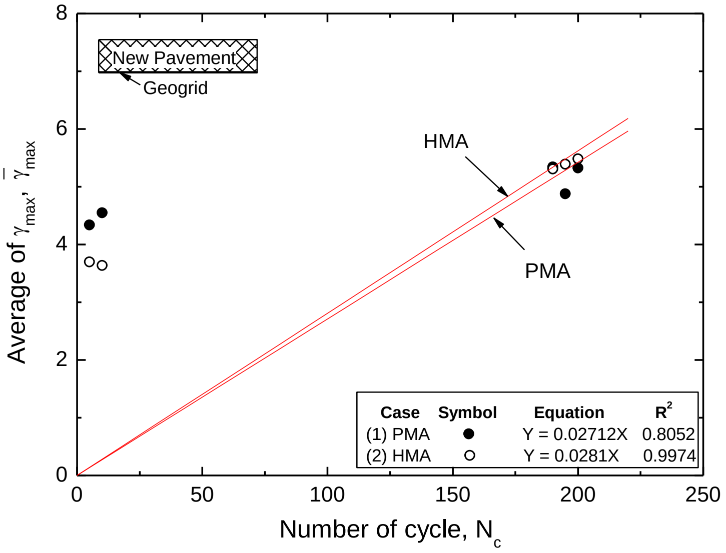

Case	Symbol	Equation	R^2
(1) PMA	●	Y = 0.02712X	0.8052
(2) HMA	○	Y = 0.0281X	0.9974

Figure 4.23(b) Relationship between average of γ_{max} and number of cycle in new reinforced with geogrid PMA and HMA pavements

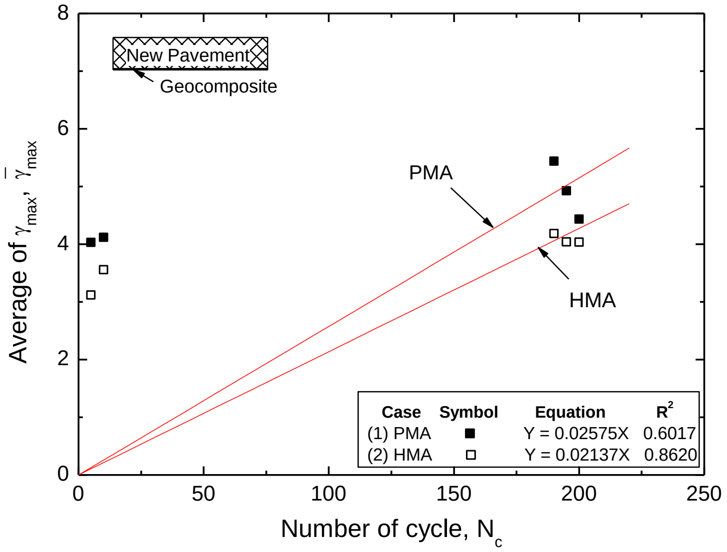

Figure 4.23(c) Relationship between average of γ_{max} and number of cycle in new reinforced with geocomposite PMA and HMA pavements

4.5.4 Surface Cracking

Figure 4.24(a) shows surface cracking in new unreinforced PMA pavement. And, Figure 4.24(b) shows surface cracking in new unreinforced HMA pavement

Figure 4.25(a) shows surface cracking in new reinforced with geogrid PMA pavement. And, Figure 4.25(b) shows surface cracking in new reinforced with geogrid HMA pavement

Figure 4.26(a) shows surface cracking in new reinforced with geocomposite PMA pavement. And, Figure 4.26(b) shows surface cracking in new reinforced with geocomposite HMA pavement

The following trends of behavior may be seen from Figure 4.24 to Figure 4.26:

1) The surface cracking significantly decreased with PMA pavement, as shown in following details:
   a) For new unreinforced PMA and HMA pavements, new unreinforced HMA pavement showed a greater degree of surface cracking. The positions of surface cracking of two cased were exhibited around the edge of model footing (dash rectangular line). For new unreinforced HMA pavement, surface cracking also propagated to top and bottom of model footing position.
   b) For new reinforced with geogrid PMA and HMA pavements, new HMA pavement reinforced with geogrid showed a greater degree of surface cracking. Three cracks were seen in HMA pavement, while two cracks were seen in PMA pavement.

c) For new PMA and HMA pavements reinforced with geocomposite, new HMA pavement reinforced with geocomposite showed a greater degree of surface cracking.

2) From the above, using of polymer modified asphalt in new pavements can decreased surface cracking.

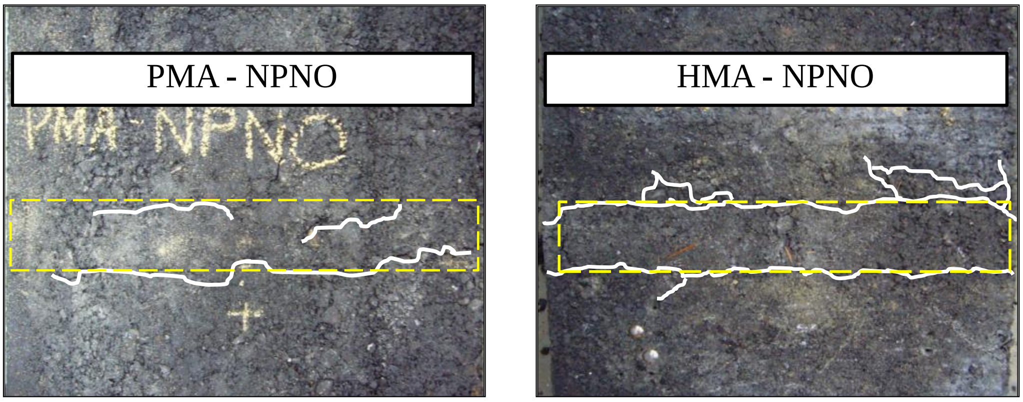

(a) (b)

Figure 4.24 Surface cracking in new unreinforced pavements: (a) PMA pavement; and (b) HMA pavement

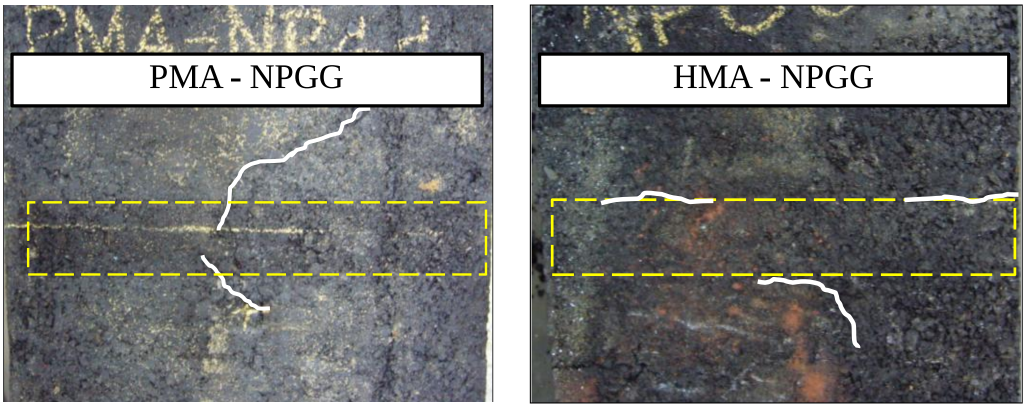

(a) (b)

Figure 4.25 Surface cracking in new reinforced with geogrid pavements: (a) PMA pavement; and (b) HMA pavement

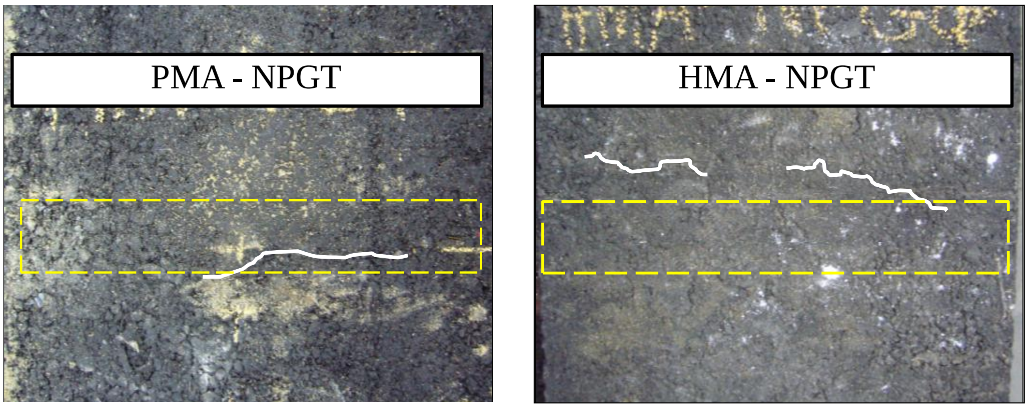

(a) (b)

Figure 4.26 Surface cracking in new reinforced with geocomposite pavements: (a) PMA pavement; and (b) HMA pavement

4.5.5 Fabric Effective Factor

From Table 4.4, FEF value for new PMA pavement reinforced with geocomposite showed a greater value among new pavement, equal to 2.79. The new HMA pavement reinforced with geocomposite, new PMA pavement reinforced with geogrid and new HMA reinforced pavement with geogrid showed a less FEF values equal to 1.65, 1.38 and 1.08, respectively. When comparing the performance of new reinforced pavements, the PMA pavement reinforced with geocomposite was the most effective for this study. Therefore, the new PMA reinforced with geocomposite would be a better choice greater choice for construction of new pavement.

Table 4.4 Fabric effectiveness factor (FEF) of new reinforced pavement between PMA and HMA pavements

Type of Reinforcement	FEF	
	PMA	HMA
Geogrid (NPGG)	1.38	1.08
Geocomposite (NPGT)	2.79	1.65

4.6 Comparisons of Overlayed Unreinforced and Reinforced Polymer Modified Asphalt (PMA) and Asphaltic Concrete (HMA) Pavements

4.6.1 Footing settlement and Footing Permanent Settlement

Figure 4.27(a) compares the relationship between the footing pressure and the footing settlement for overlayed unreinforced PMA and HMA pavements. Figure 4.27(b) compares the relationship between the footing pressure and the footing settlement for overlayed PMA and HMA pavements reinforced with geogrid. Figure 4.27(c) compares the relationship between the footing pressure and the footing settlement for overlayed PMA and HMA pavements reinforced with geocomposite. And, Figure 4.27(d) compares the relationship between the footing pressure and the footing settlement for overlayed PMA and HMA pavements reinforced with geogrid together with geocomposite.

Figure 4.28(a) compares the relationship between the footing settlement and the elapsed time for overlayed unreinforced PMA and HMA pavements, Figure 4.28(b) compares the relationship between the footing settlement and the elapsed time for overlayed PMA and HMA pavements reinforced with geogrid, Figure 4.28(c) compares the relationship between the footing settlement and the elapsed time for overlayed PMA and HMA pavements reinforced with geocomposite. And, Figure 4.28(d) compares the relationship between the footing settlement and the elapsed time for overlayed PMA and HMA pavements reinforced with geogrid together with geocomposite.

Figure 4.29(a) compares the relationship between the permanent settlement of footing and the number of cycles of cyclic loading for overlayed unreinforced PMA and HMA pavements. Figure 4.29(b) compares the relationship between the permanent settlement of footing and the number of cycles of cyclic loading for overlayed PMA and HMA pavements reinforced with geogrid. Figure 4.29(c) compares the relationship between the permanent settlement of footing and a number of cycles of cyclic loading in overlayed PMA and HMA pavements reinforced with geocomposite. And, Figure 4.29(d) compares a relationship between a permanent settlement of footing and a number of cycles of cyclic loading in overlayed PMA and HMA pavements reinforced with geogrid together with geocomposite.

Table 4.5 shows the ratios of permanent settlement of footing between overlayed PMA and HMA pavements.

The following trends of behavior may be seen from Figure 4.27-Figure 4.29 and Table 4.5:

1) Both the footing settlement and the footing permanent settlement increased with an increase in the number of cycle of cyclic loading, the footing pressure and the elapsed time.
2) The footing settlement and the permanent settlement of the footing were significantly decreased in PMA pavement, as seen in following details:
   a) For overlayed unreinforced PMA and HMA pavements, overlayed unreinforced HMA pavement showed a greater footing settlement and the permanent settlement of the footing when compared at the same time.
   b) For overlayed PMA and HMA pavements reinforced with geogrid, overlayed reinforced with geogrid HMA pavement showed a greater footing settlement and the permanent settlement of the footing when compared at the same time.
   c) For overlayed PMA and HMA pavements reinforced with geocomposite, overlayed reinforced with geocomposite HMA pavement showed a greater footing settlement and the permanent settlement of the footing when compared at the same time.
   d) For overlayed PMA and HMA pavements reinforced with geogrid together with geocomposite, overlayed HMA reinforced with geogrid together with geocomposite pavement showed a greater footing settlement

and the permanent settlement of the footing when compared at the same time.

3) When comparing the permanent settlement of footing at 200 cycles of cyclic loading between overlayed PMA and HMA pavements, the ratio of the values of overlayed unreinforced, HMA pavement reinforced with geogrid, HMA pavement reinforced with geocomposite and HMA pavement reinforced with geogrid together with geocomposite were equal to 1.81, 1.27, 1.29 and 1.05, respectively. Thus, the overlayed PMA pavements were more effective in resisting permanent settlement of footing than the overlayed HMA pavements.

4.) The rate of footing permanent settlement development decreased with an increase in the number of cycle of cyclic loading. That is, the footing permanent settlement relatively largerly occurred in the first section of loading (approximate $N_c = 1$ to $N_c = 50$). Then, plastic deformation (irreversible deformation) occurred in some area of pavement structure underneath the footing model. After that, the footing permanent settlement relative less occurred and became stable in the last section of loading. Due to occurrence of plastic deformation in the first section of loading, the plastic deformation was less distributed to new area of pavement.

5.) From the above, using PM-AC in overlayed pavements was able to decreased permanent settlement of footing. And, the polymer modification could increase stiffness (hardness) of pavement. Therefore, the overlayed PMA pavement may be less sensitive to occurrence permanent settlement.

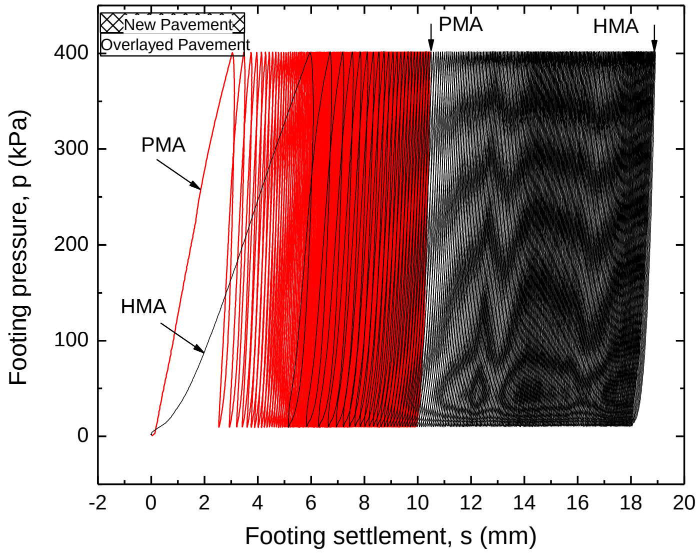

Figure 4.27(a) Relationship between footing pressure and footing settlement in overlayed unreinforced PMA and HMA pavements

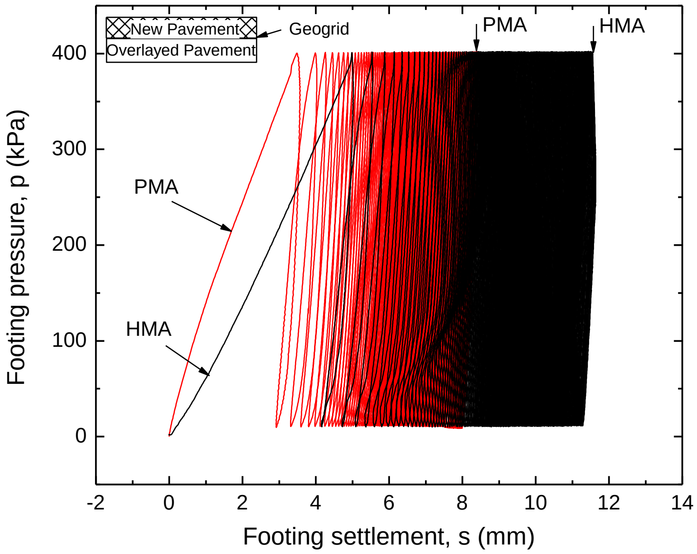

Figure 4.27(b) Relationship between footing pressure and footing settlement in overlayed PMA and HMA pavements reinforced with geogrid

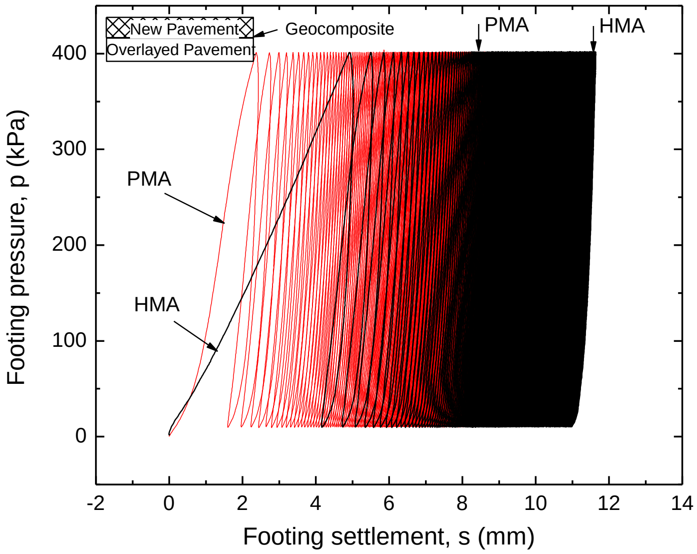

Figure 4.27(c) Relationship between footing pressure and footing settlement in overlayed PMA and HMA pavements reinforced with geocomposite

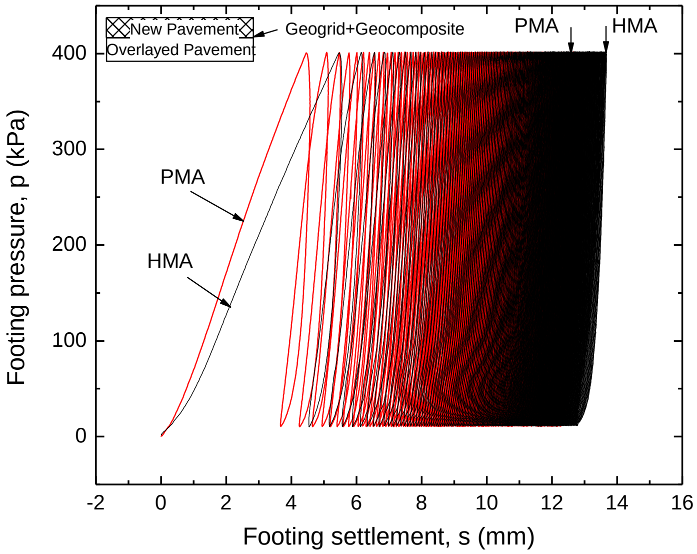

Figure 4.27(d) Relationship between footing pressure and footing settlement in overlayed PMA and HMA pavements reinforced with geogrid together with geocomposite

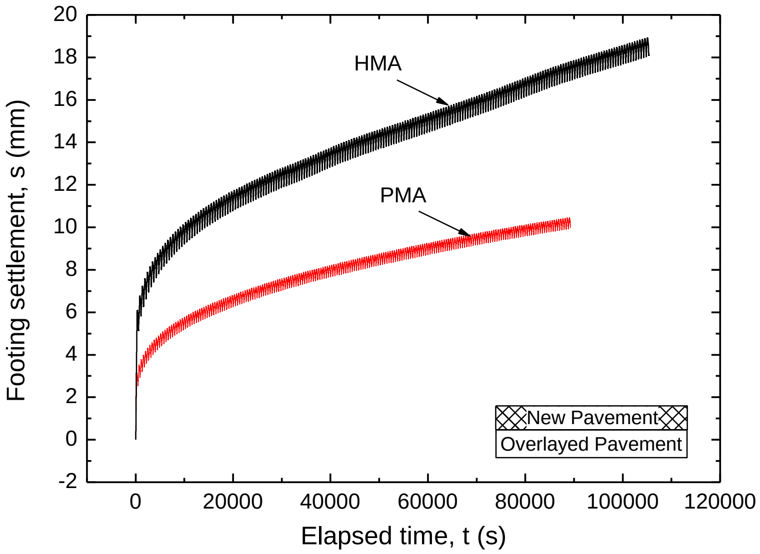

Figure 4.28(a) Relationship between footing settlement and elapsed time for overlayed unreinforced PMA and HMA pavements

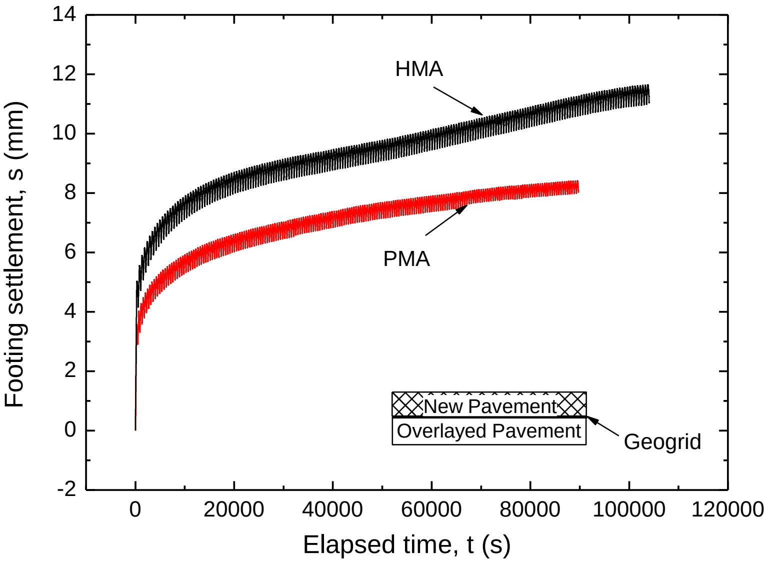

Figure 4.28(b) Relationship between footing settlement and elapsed time for overlayed PMA and HMA pavements reinforced with geogrid

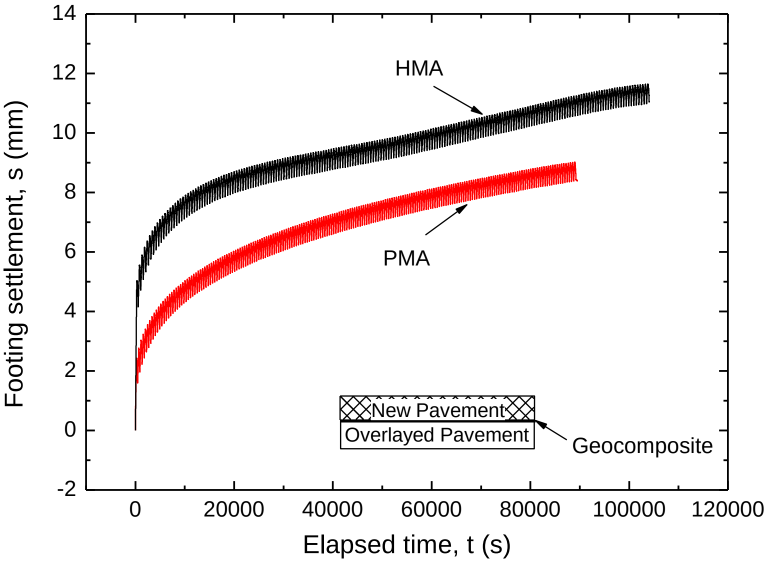

Figure 4.28(c) Relationship between footing settlement and elapsed time for overlayed PMA and HMA pavements reinforced with geocomposite

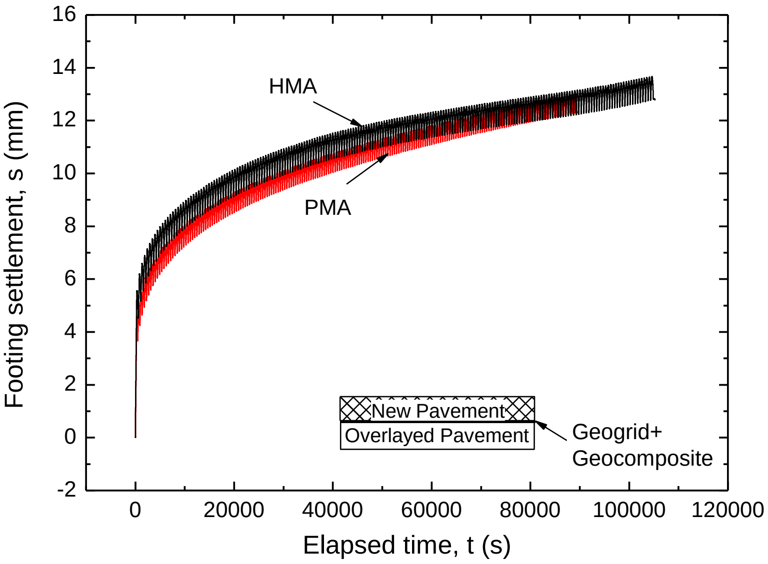

Figure 4.28(d) Relationship between footing settlement and elapsed time for overlayed PMA and HMA pavements reinforced with geogrid together with geocomposite

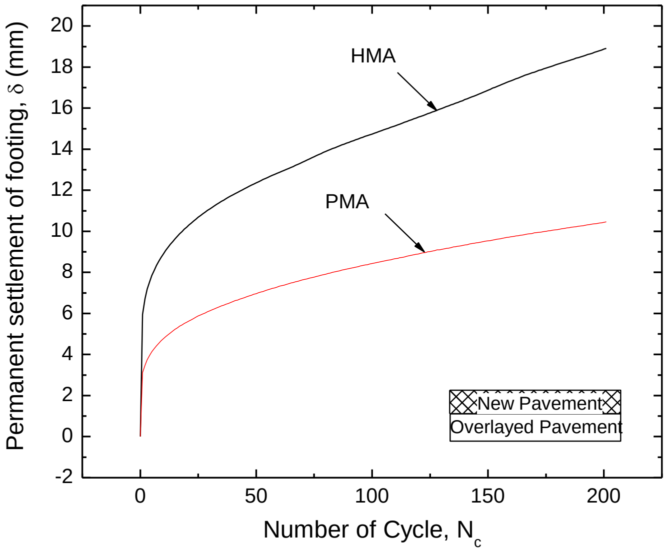

Figure 4.29(a) Relationship between permanent settlement of footing settlement and number of cycle for overlayed unreinforced PMA and HMA pavements

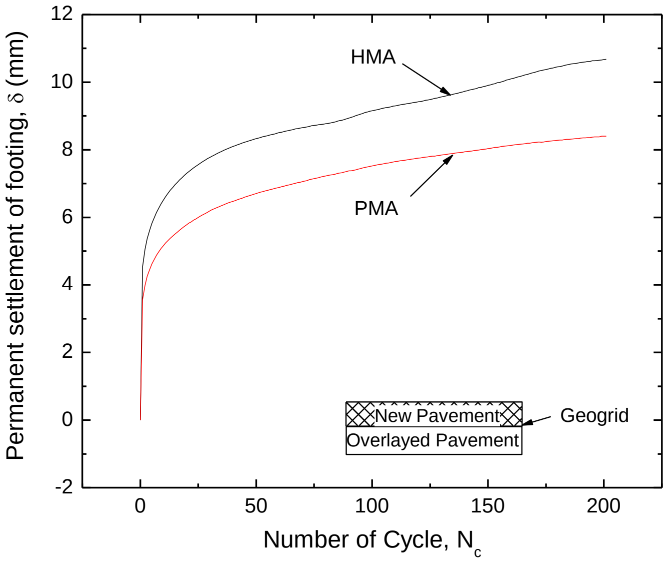

Figure 4.29(b) Relationship between permanent settlement of footing settlement and number of cycle for overlayed PMA and HMA pavements reinforced with geogrid

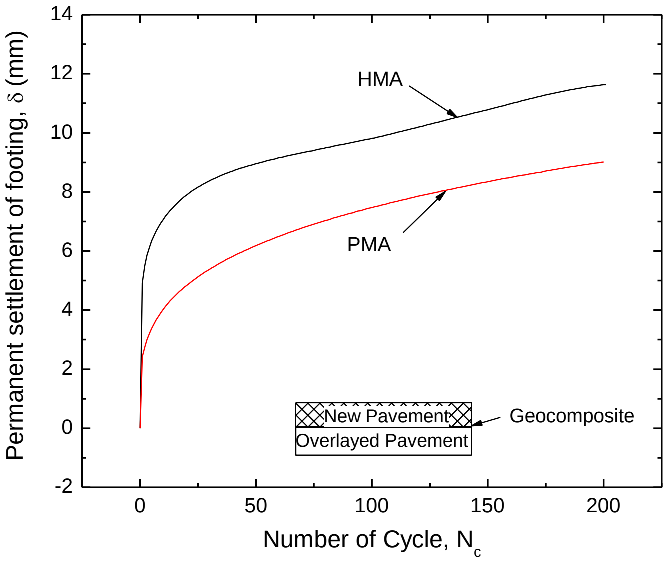

Figure 4.29(c) Relationship between permanent settlement of footing settlement and number of cycle for overlayed PMA and HMA pavements reinforced with geocomposite

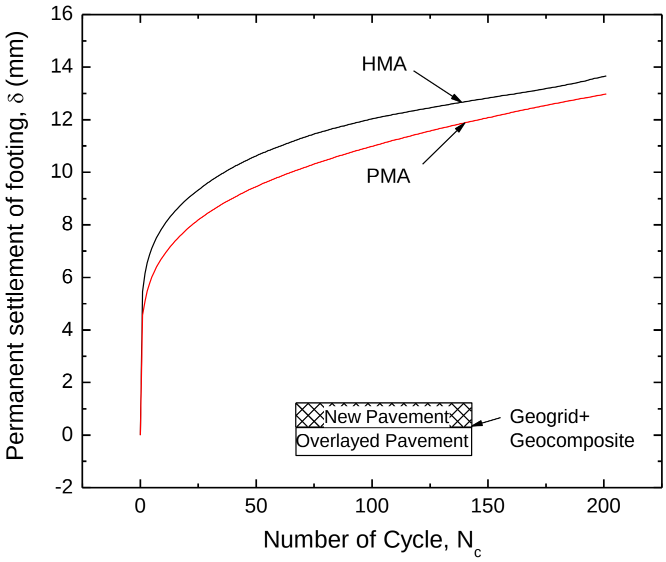

Figure 4.29(d) Relationship between permanent settlement of footing settlement and number of cycle for overlayed PMA and HMA pavements reinforced with geogrid together with geocomposite

Table 4.5 Ratio of permanent settlement of footing between overlayed PMA and HMA pavements at 200 cycles of cyclic loading

Type of Reinforcement	**Ratio of permanent settlement of footing between new PMA and HMA pavements** $(\frac{\delta_{HMA}}{\delta_{PMA}})$ **at 200 cycles of cyclic loading**
Unreinforced (DMNO)	1.81
Reinforced with geogrid (DMGG)	1.27
Reinforced with geocomposite (DMGT)	1.29
Reinforced with geogrid together with geocomposite (DMGGGT)	1.05

4.6.2 Surface Settlement and Settlement Underneath Pavement

Figure 4.30(a) compares the relationship between the surface settlement and the distance from center of footing at different numbers of cycle for overlayed unreinforced PMA and HMA pavements. Figure 4.30(b) compares the relationship between the surface settlement and the distance from center of footing at different numbers of cycle for overlayed PMA and HMA pavements reinforced with geogrid. Figure 4.30(c) compares the relationship between the surface settlement and the distance from center of footing at different numbers of cycle for overlayed PMA and HMA pavements reinforced with geocomposite. And, Figure 4.30(d) compares the relationship between the surface settlement and the distance from center of footing at different numbers of cycle for overlayed PMA and HMA pavements reinforced with geogrid together with geocomposite.

Figure 4.31(a) compares the settlement underneath asphalt pavement at different numbers of cycle for overlayed unreinforced PMA and HMA pavements. Figure 4.31(b) compares a settlement underneath asphalt pavement at different numbers of cycle for overlayed PMA and HMA pavements reinforced with geogrid. Figure 4.31(c) compares a settlement underneath asphalt pavement at different numbers of cycle for overlayed PMA and HMA pavements reinforced with geocomposite. And, Figure 4.31(d) compares a settlement underneath asphalt pavement at different numbers of cycle for overlayed PMA and HMA pavements reinforced with geogrid together with eocomposite.

The following trends of behavior may be seen from Figure 4.30 and Figure 4.31:

1) Both the surface settlement and the settlement underneath asphalt pavement increased with an increase in the number of cycle of cyclic loading.
2) On the other hand, both the surface settlement and the settlement underneath asphalt pavement decreased with an increasing in the distance from center of footing.
3) The surface settlement was significantly decreased in PMA pavement, as seen in following details:
   a) For overlayed unreinforced PMA and HMA pavements, overlayed unreinforced HMA pavement showed a greater footing surface settlement when compared at the same cycle of cyclic loading.
   b) For overlayed PMA and HMA pavements reinforced with geogrid, overlayed HMA pavement reinforced with geogrid showed a greater footing surface settlement when compared at the same cycle of cyclic loading.
   c) For overlayed PMA and HMA pavements reinforced with geocomposite, overlayed HMA pavement reinforced with geocomposite showed a greater footing surface settlement when compared at the same cycle of cyclic loading.
   d) For overlayed PMA and HMA pavements reinforced with geogrid together with geocomposite, overlayed HMA pavement reinforced with geogrid together with geocomposite showed a greater footing surface settlement when compared at the same cycle of cyclic loading.
4) The behaviors settlement underneath pavement were varied for different pavements, as shown in following details:

a) For overlayed unreinforced PMA and HMA pavements, overlayed unreinforced HMA pavement showed a greater settlement underneath pavement when compared at the same cycle of cyclic loading.

b) For overlayed PMA and HMA pavements reinforced with geogrid, the settlement underneath pavements for PMA pavement and HMA pavement were quite similar.

c) For overlayed PMA and HMA pavements reinforced with geocomposite, overlayed PMA pavement reinforced with geocomposite showed a greater footing surface settlement when compared at the same cycle of cyclic loading.

d) For overlayed PMA and HMA pavements reinforced with geogrid together with geocomposite, overlayed HMA pavement reinforced with geogrid together with geocomposite showed a greater settlement underneath pavement when compared at the same cycle of cyclic loading.

5) Trends of surface settlement were different between PMA and HMA pavements in the first section of loading (N_c = 5 and N_c = 10) and the last section of loading (N_c = 190, N_c = 195 and N_c = 200). For overlayed PMA pavements, the direction of surface settlement and settlement underneath pavement were downward for all the distances from the center of model footing. On the other hand, for overlayed HMA pavements, the direction of surface settlement and settlement underneath pavement were downward at locations near the model footing center; but, they were upward at approximately 100 mm from the model footing center.
6) Trends of settlement underneath pavement were similar between PMA and HMA pavements in the first section of loading (N_c = 5 and N_c = 10) and the last section of loading (N_c = 190, N_c = 195 and N_c = 200).
7) From the above, the overlayed HMA pavements showed a greater bending moment stabilized in pavements. Thus, the overlayed PMA pavements were able to decrease bending moment in pavements. The cracking in overlayed PMA pavements may be less developed.

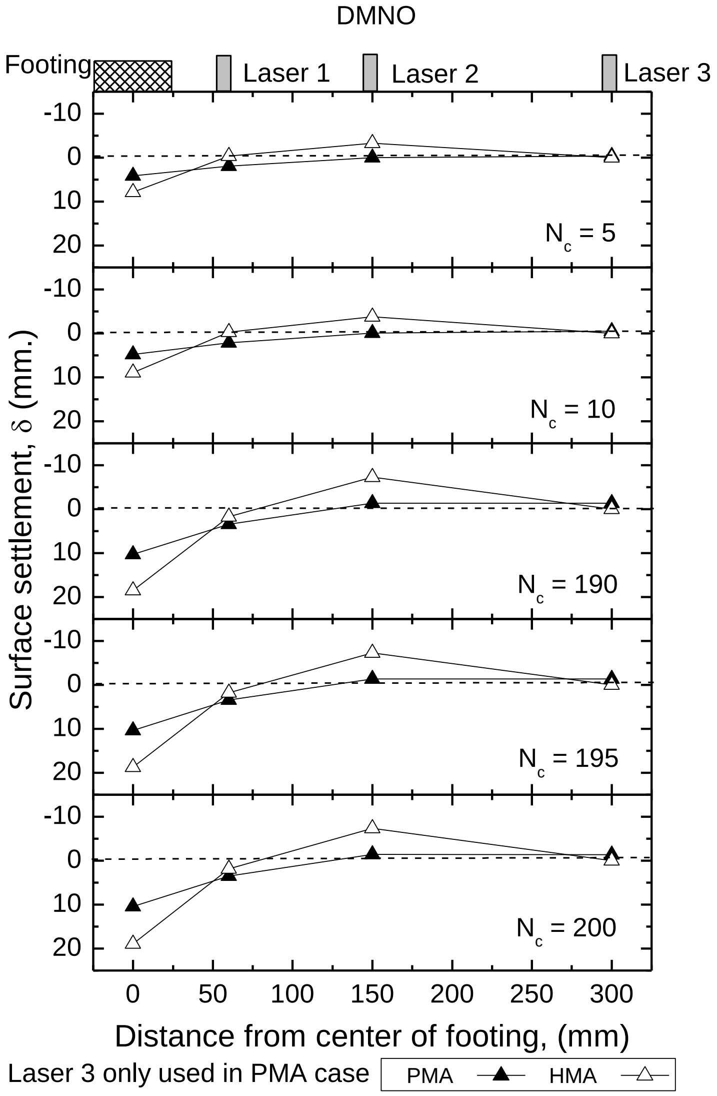

Figure 4.30(a) Relationship between surface settlement and distance from center of footing in overlayed unreinforced PMA and HMA pavements

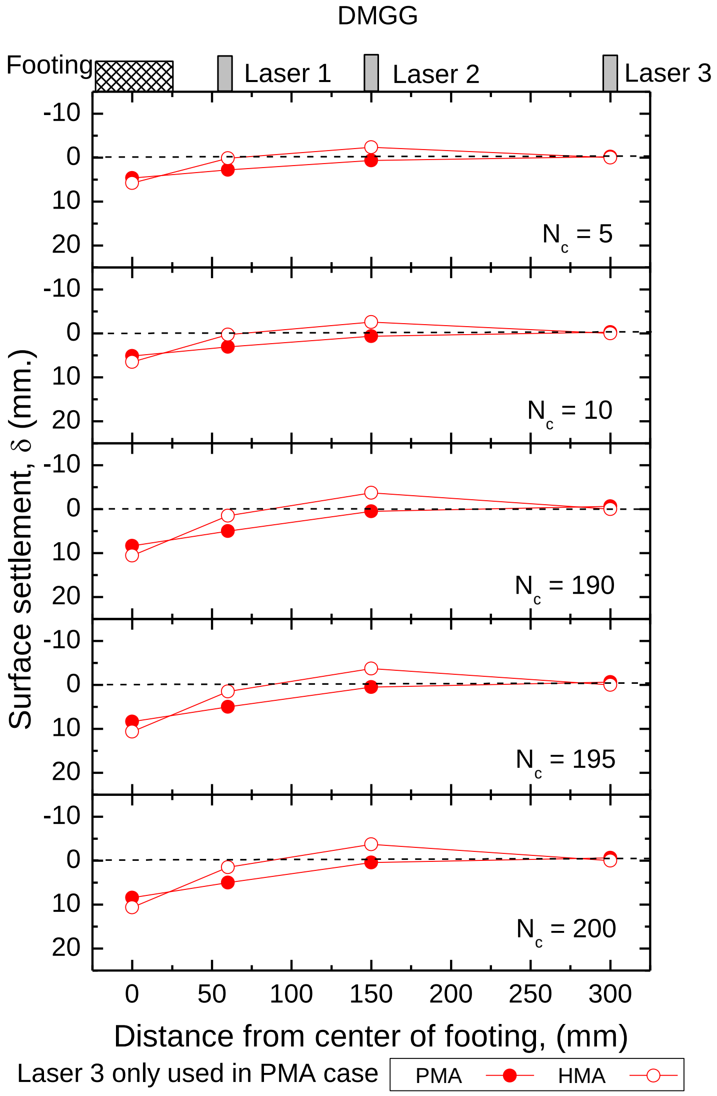

Figure 4.30(b) Relationship between surface settlement and distance from center of footing in overlayed PMA and HMA pavements reinforced with geogrid

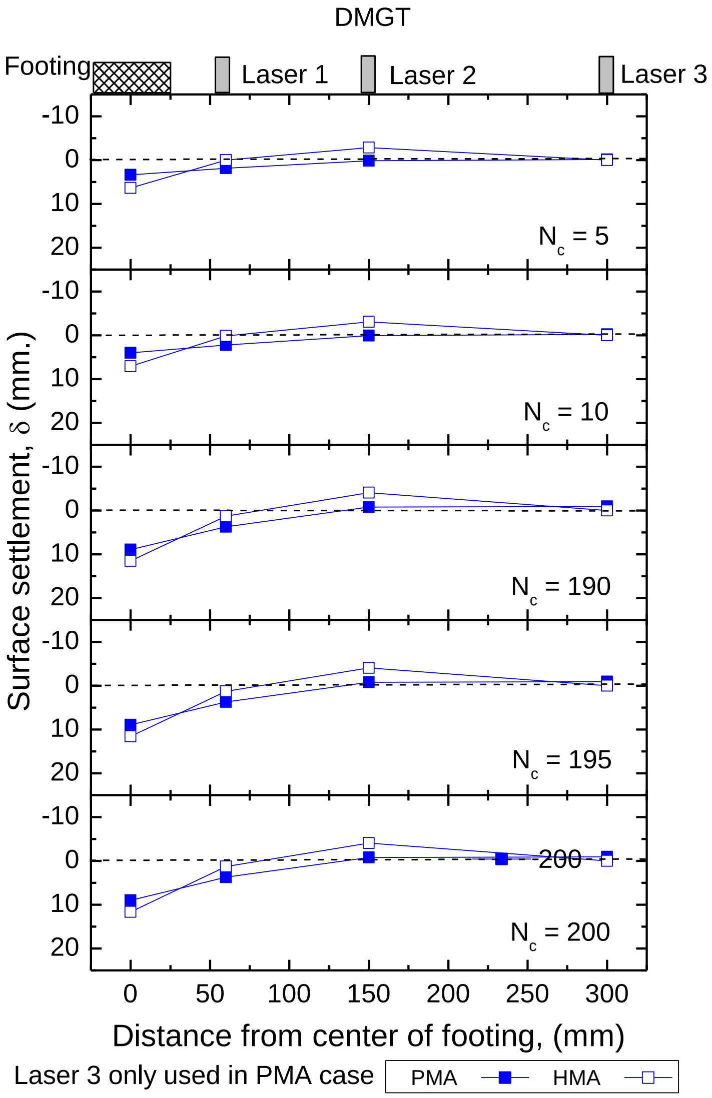

Figure 4.30(c) Relationship between surface settlement and distance from center of footing in overlayed PMA and HMA pavements reinforced with geocomposite

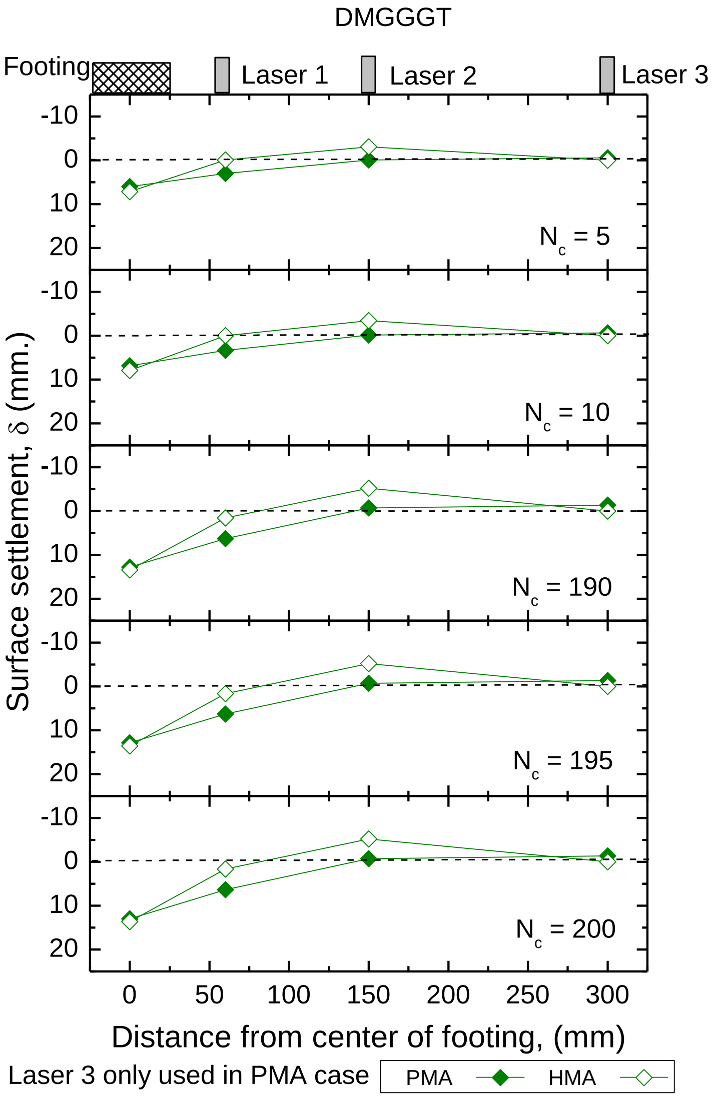

Figure 4.30(d) Relationship between surface settlement and distance from center of footing in overlayed PMA and HMA pavements reinforced with geogrid together with geocomposite

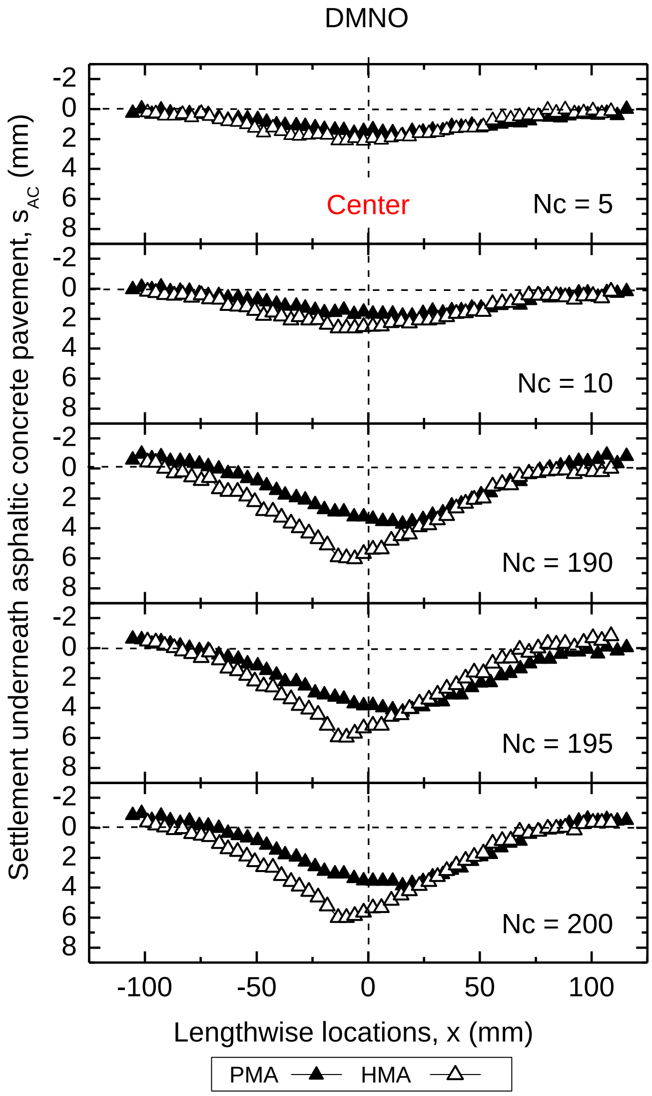

Figure 4.31(a) Settlement underneath asphalt pavement in overlayed unreinforced PMA and HMA pavements

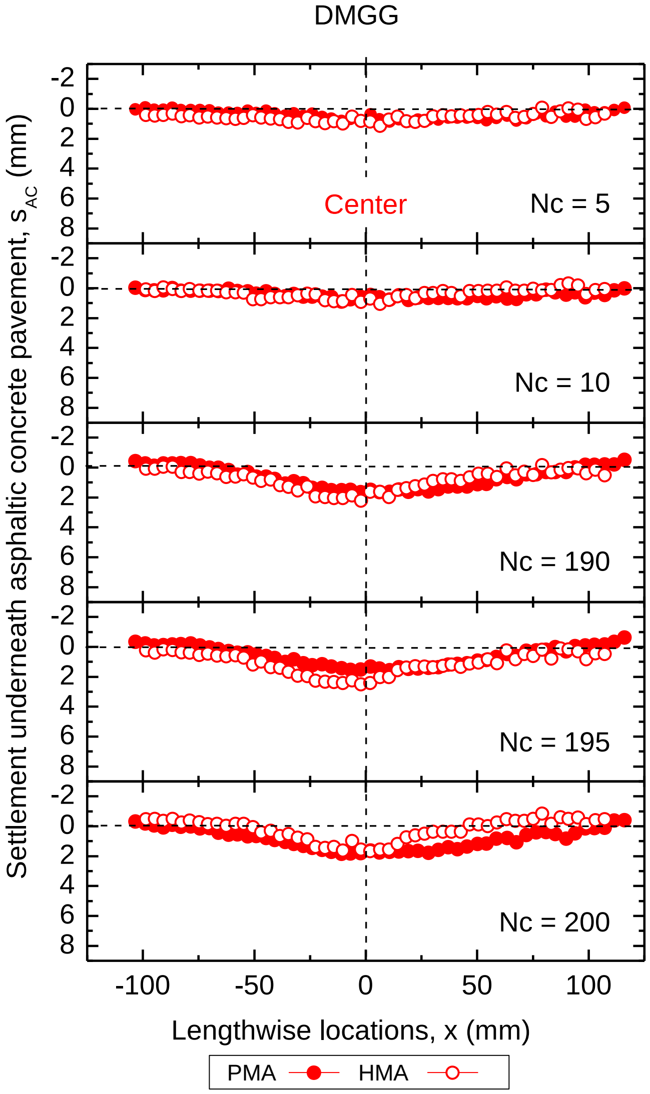

Figure 4.31(b) Settlement underneath asphalt pavement in overlayed PMA and HMA pavements reinforced with geogrid

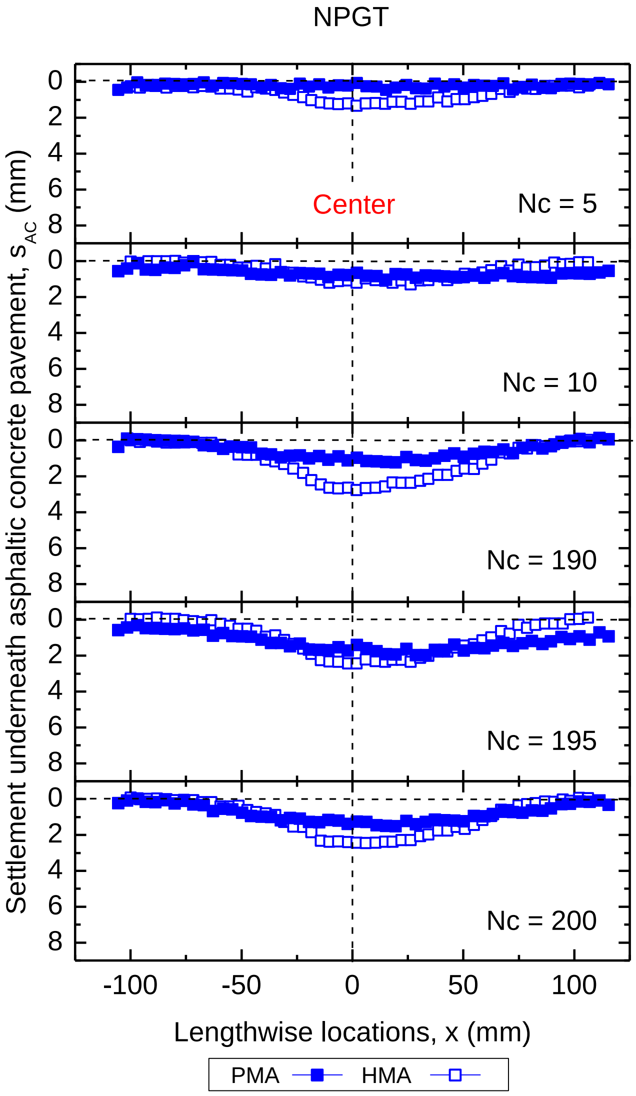

Figure 4.31(c) Settlement underneath asphalt pavement in overlayed PMA and HMA pavements reinforced with geocomposite

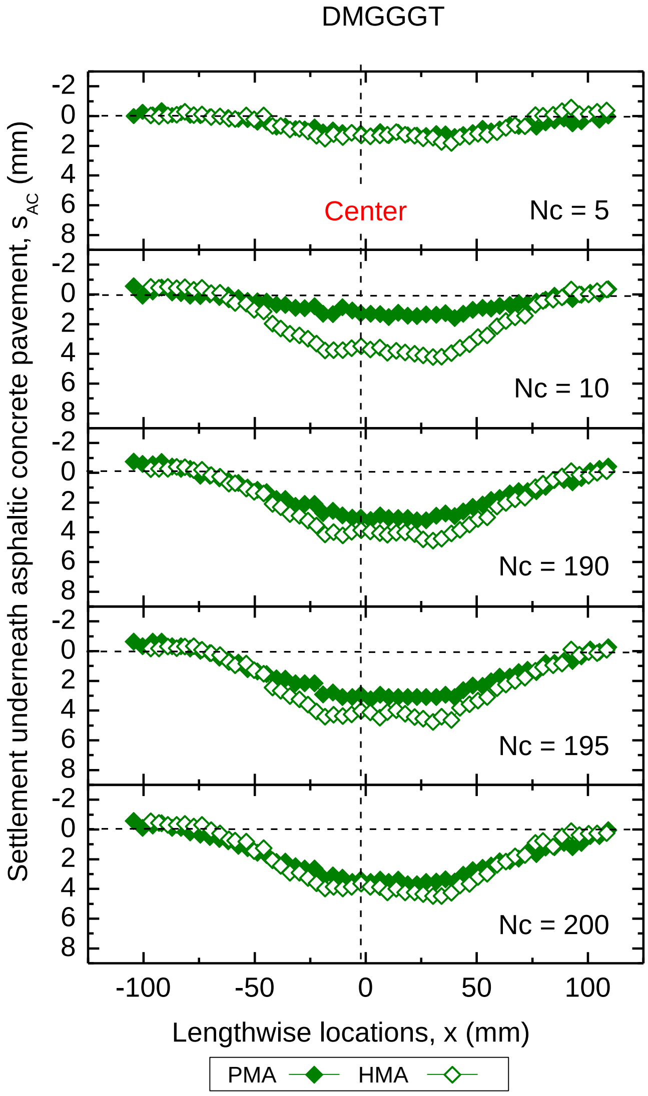

Figure 4.31(d) Settlement underneath asphalt pavement in overlayed PMA and HMA pavements reinforced with geogrid together with geocomposite

4.6.3 Strain Field of Sand Subbase

Figure 4.32(a) shows maximum shear strain ($\gamma_{\max}$) distribution in overlayed unreinforced PMA pavement at 200 cycles of cyclic loading and Figure 4.32(b) shows maximum shear strain ($\gamma_{\max}$) distribution in overlayed unreinforced HMA pavement at 200 cycles of cyclic loading.

Figure 4.33(a) shows maximum shear strain ($\gamma_{\max}$) distribution in overlayed PMA pavement reinforced with geogrid at 200 cycles of cyclic loading and Figure 4.33(b) shows maximum shear strain ($\gamma_{\max}$) distribution in overlayed HMA pavement reinforced with geogrid at 200 cycles of cyclic loading.

Figure 4.34(a) shows maximum shear strain ($\gamma_{\max}$) distribution in overlayed PMA pavement reinforced with geocomposite at 200 cycles of cyclic loading and Figure 4.34(b) shows maximum shear strain ($\gamma_{\max}$) distribution in overlayed HMA pavement reinforced with geocomposite at 200 cycles of cyclic loading.

Figure 4.35(a) shows maximum shear strain ($\gamma_{\max}$) distribution in overlayed PMA pavement reinforced with geogrid together with geocomposite at 200 cycles of cyclic loading and Figure 4.35(b) shows maximum shear strain ($\gamma_{\max}$) distribution in overlayed HMA pavement reinforced with geogrid together with geocomposite at 200 cycles of cyclic loading.

Figure 4.36(a) shows relationship between average of $\gamma_{\max}$ and number of cycle in overlayed unreinforced PMA and HMA pavements. Figure 4.36(b) shows relationship between average of $\gamma_{\max}$ and number of cycle in overlayed reinforced with geogrid PMA and HMA pavements. Figure 4.36(c) shows relationship between average of $\gamma_{\max}$ and number of cycle in overlayed reinforced with geocomposite PMA and HMA pavements. Figure 4.36(d) shows relationship between average of $\gamma_{\max}$ and number of cycle in overlayed reinforced with geogrid with geocomposite PMA and HMA pavements.

The following trends of behavior may be seen from Figure 4.32 and Figure 4.36:

1) The maximum shear strain ($\gamma_{\max}$) distribution significantly decreased with PMA pavement, as shown in following details:
    a) For overlayed unreinforced PMA and HMA pavements, overlayed unreinforced HMA pavement showed a greater maximum shear strain ($\gamma_{\max}$) distribution. The shear band can be clearly seen in HMA pavement.
    b) For overlayed PMA and HMA pavements reinforced with geogrid, overlayed HMA pavements reinforced with geogrid showed a greater maximum shear strain ($\gamma_{\max}$) distribution. The shear band can be rather seen in HMA pavement.
    c) For overlayed PMA and HMA pavements reinforced with geocomposite, the maximum shear strain ($\gamma_{\max}$) distributions were similar in both PMA pavements and HMA pavements.

d) For overlayed PMA and HMA pavements reinforced with geogrid together with geocomposite, overlayed e HMA pavements reinforced with geogrid together with geocomposithas showed a greater maximum shear strain ($\gamma_{\max}$) distribution. The shear band can be clearly seen in HMA pavement.

2) The rate of maximum shear strain ($\gamma_{\max}$) development significantly decreased PMA pavement, as shown in following details:

   a) For overlayed unreinforced PMA and HMA pavements, rate of maximum shear strain ($\gamma_{\max}$) development value much differed between PMA pavement and HMA pavement, approximate to 0.01 %/cycle, by overlayed unreinforced HMA pavement showed a greater rate of maximum shear strain ($\gamma_{\max}$) development.

   b) For overlayed reinforced with geogrid PMA and HMA pavements, overlayed PMA pavement reinforced with geogrid showed a greater rate of maximum shear strain ($\gamma_{\max}$) development.

   c) For overlayed reinforced with geocomposite PMA and HMA pavements, overlayed PMA pavement reinforced with geocomposite showed a greater rate of maximum shear strain ($\gamma_{\max}$) development.

   d) For overlayed reinforced with geogrid together with geocomposite PMA and HMA pavements, rate of maximum shear strain ($\gamma_{\max}$) development value much differed between PMA pavement and HMA pavement, approximate to 0.008 %/cycle, by overlayed reinforced with geogrid together with geocomposite HMA pavement showed a greater rate of maximum shear strain ($\gamma_{\max}$) development.

3) From the above, the maximum shear strain ($\gamma_{\max}$) distributions were greater seen in overlayed HMA pavements. The subbase may be failed along direction of the maximum shear strain ($\gamma_{\max}$) distribution. Therefore, the overlayed PMA pavements were able to decrease susceptibility to failure in subbase pavement.

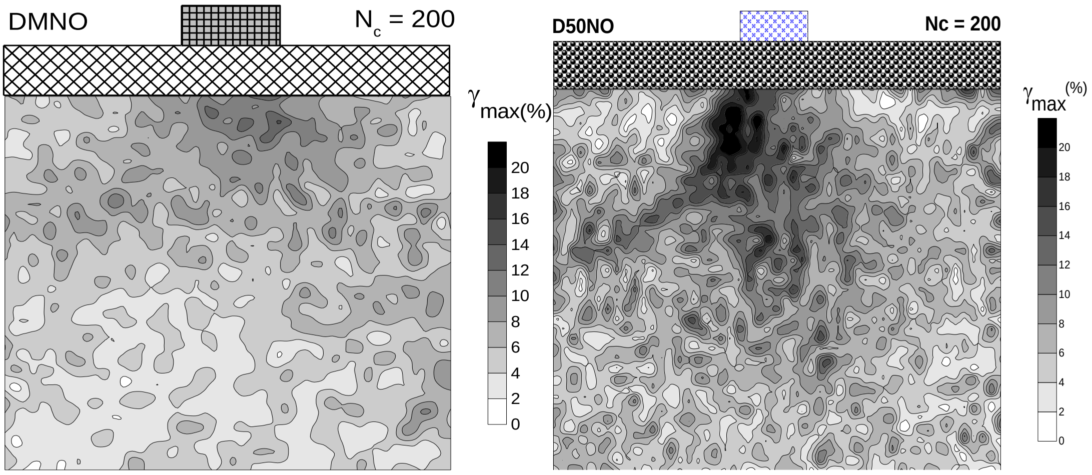

(a) (b)

Figure 4.32 Maximum shear strain distribution in overlayed unreinforced pavements at 200 cycles of cyclic loading; (a) PMA pavement and (b) HMA pavement

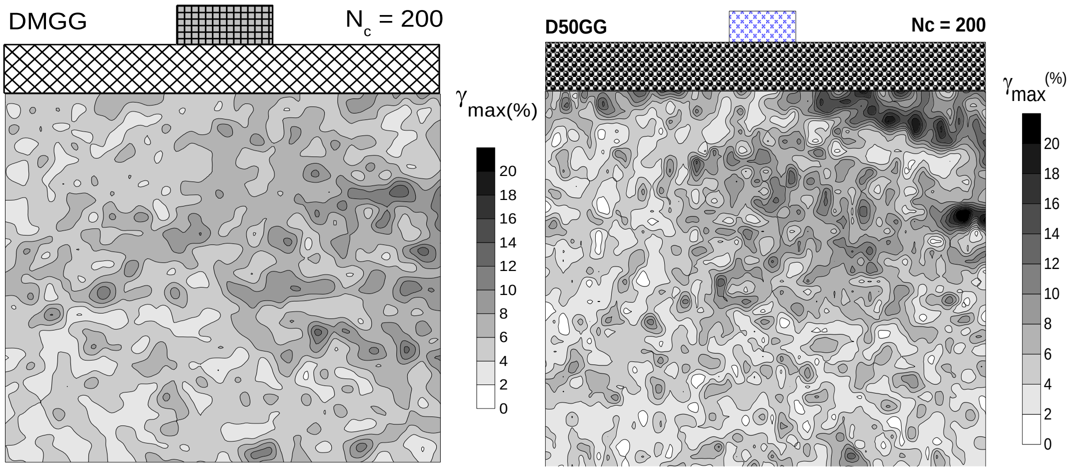

(a) (b)

Figure 4.33 Maximum shear strain distribution in overlayed pavements reinforced with geogrid at 200 cycles of cyclic loading; (a) PMA pavement and (b) HMA pavement

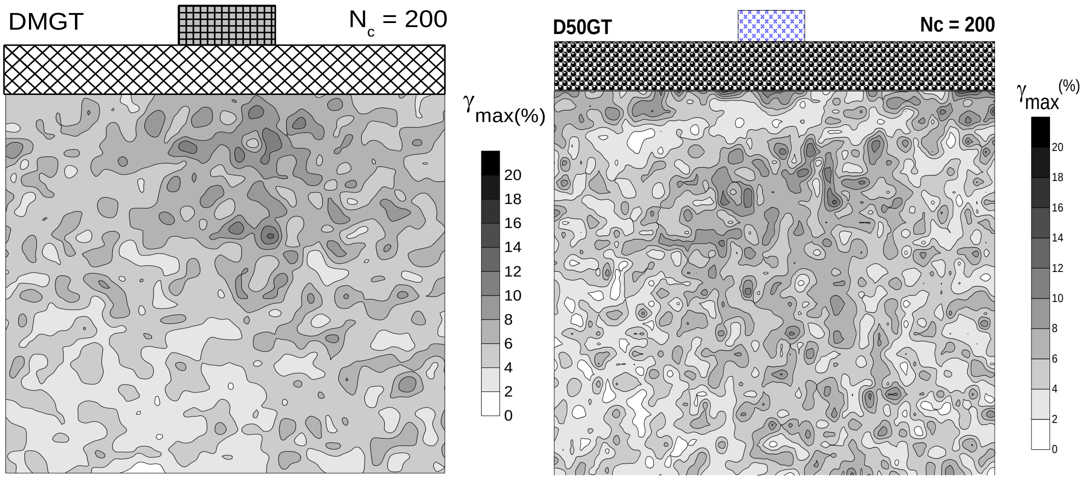

(a) (b)

Figure 4.34 Maximum shear strain distribution in overlayed pavements reinforced with geocomposite at 200 cycles of cyclic loading; (a) PMA pavement and (b) HMA pavement

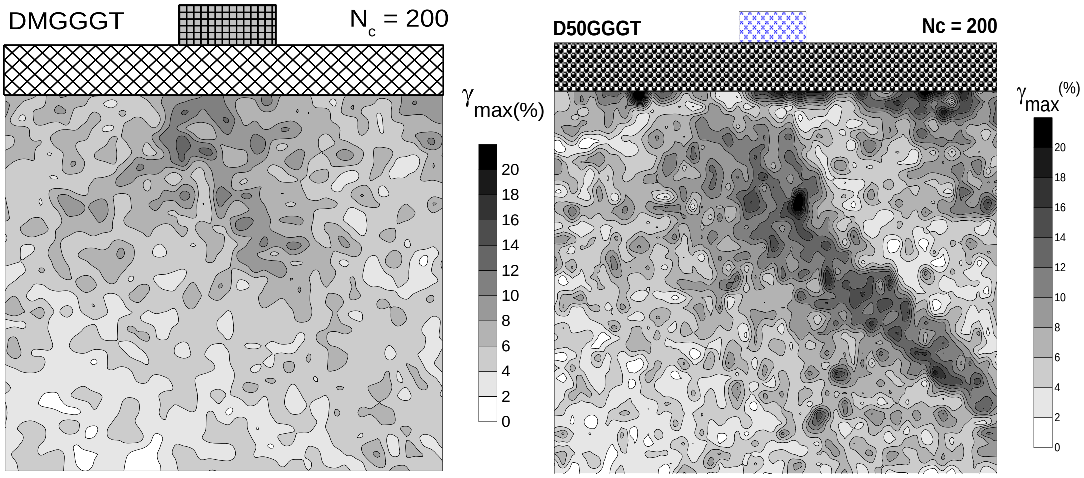

(a) (b)

Figure 4.35 Maximum shear strain distribution in overlayed pavements reinforced with geogrid together with geocomposite at 200 cycles of cyclic loading; (a) PMA pavement and (b) HMA pavement

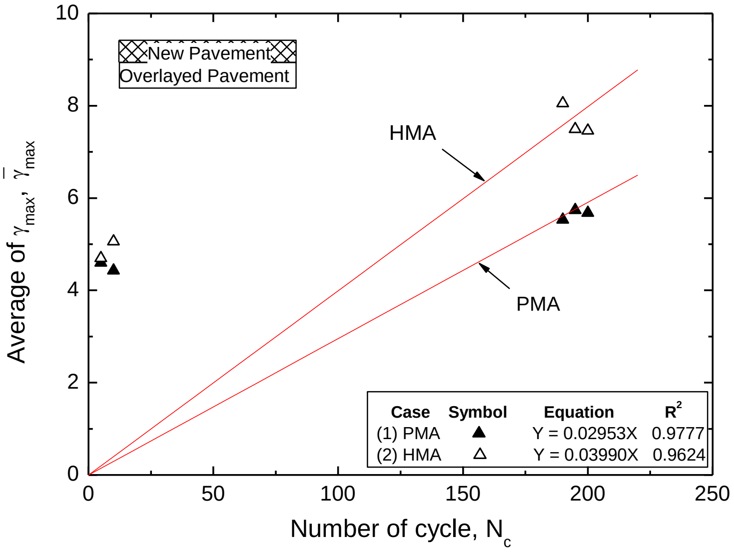

Figure 4.36(a) Relationship between average of γ_{max} and number of cycle in overlayed unreinforced PMA and HMA pavements

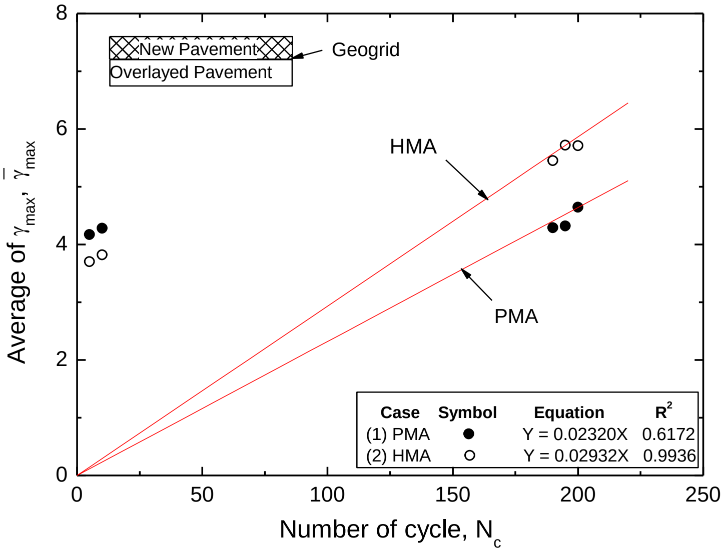

Figure 4.36(b) Relationship between average of γ_{max} and number of cycle in overlayed reinforced with geogrid PMA and HMA pavements

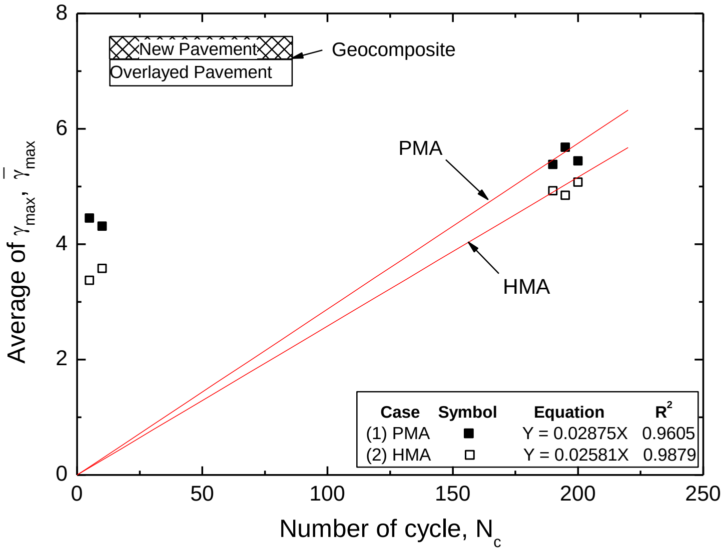

Figure 4.36(c) Relationship between average of γ_{max} and number of cycle in overlayed reinforced with geocomposite PMA and HMA pavements

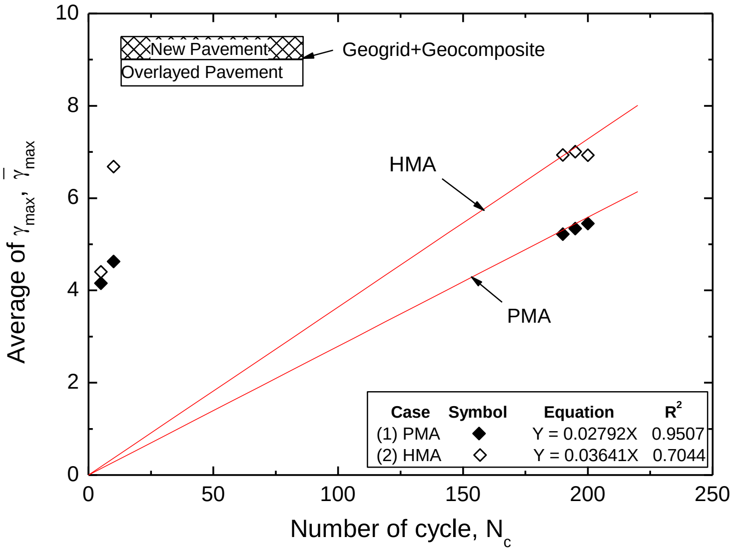

Figure 4.36(d) Relationship between average of γ_{max} and number of cycle in overlayed reinforced with geogrid together with geocomposite PMA and HMA pavements

4.6.4 Surface Cracking

Figure 4.37(a) shows surface cracking in overlayed reinforced with geocomposite PMA pavement. And, Figure 4.37(b) shows surface cracking in overlayed reinforced with geocomposite HMA pavement

Figure 4.38(a) shows surface cracking in overlayed reinforced with geogrid together with geocomposite PMA pavement. And, Figure 4.38(b) shows surface cracking in overlayed reinforced with geogrid together with geocomposite HMA pavement

For overlayed unreinforced and reinforced with geogrid PMA and HMA pavements, unreinforced and overlayed reinforced with HMA pavements were not found. Thus, comparisons of these cases were not showed in this study.

The following trends of behavior may be seen from Figure 4.37 to Figure 4.38:

1) The surface cracking significantly decreased with PMA pavement, as shown in following details:
   a) For overlayed reinforced with geocomposite PMA and HMA pavements, overlayed reinforced with geocomposite PMA pavement showed a greater degree of surface cracking. The positions of surface cracking of two cased were exhibited around the edge of model footing (dash rectangular line).
   b) For overlayed reinforced with geogrid and geocomposite PMA and HMA pavements, overlayed HMA pavement reinforced with geogrid and geocomposite showed a greater degree of surface cracking.
2) From the above, the results from two cases were different. Therefore, occurring of surface cracking for overlayed PMA and HMA pavements was not summarized in this study.

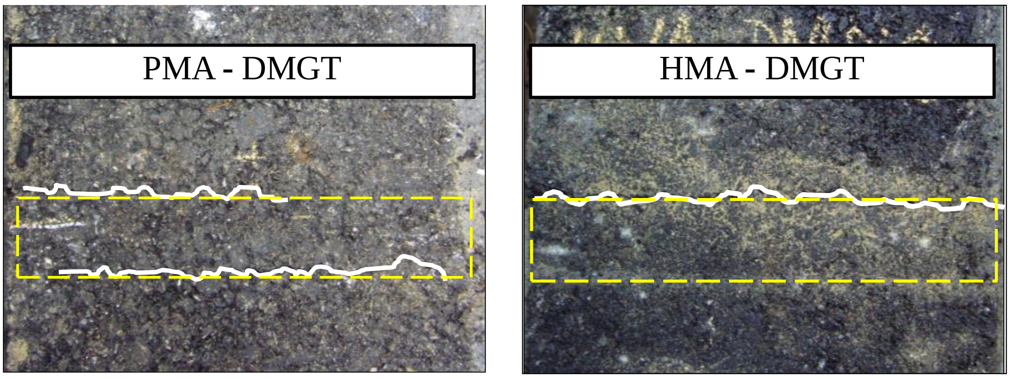

(a) (b)

Figure 4.37 Surface cracking in overlyed reinforced with geocomposite pavements: (a) PMA pavement; and (b) HMA pavement

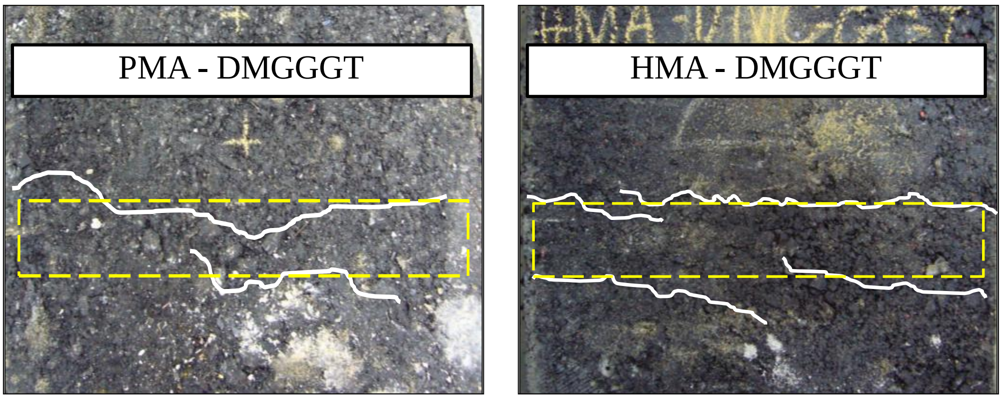

(a) (b)

Figure 4.38 Surface cracking in overlyed reinforced with geogrid together with geocomposite pavements: (a) PMA pavement; and (b) HMA pavement

4.6.5 Fabric Effective Factor

From Table 4.6, FEF value in overlayed reinforced PMA pavement and HMA pavement with geogrid showed the greatest value among overlayed pavements, equal to 1.24 and 1.77, respectively. The overlayed PMA and HMA pavement reinforced with geogrid together with geocomposite showed the lowest value among overlayed pavements, equal to 0.81 and 1.38, respectively. When comparing the performance of overlayed reinforced pavement, the pavement with reinforced geogrid was the most effective for this study.

Table 4.6 Fabric effectiveness factor (FEF) of overlayed reinforced pavement between PMA and HMA pavements

Type of Geosynthetics	**FEF**	
	PMA	**HMA**
Geogrid (DMGG)	1.24	1.77
Geocomposite (DMGT)	1.26	1.63
Geogrid+ Geocomposite (DMGGGT)	0.81	1.38

4.7 Comparisons of Polymer Modified Asphalt Cement (PM-AC) and Geosynthetics

The increased performances in pavement can be calculated by comparing the permanent settlement of footing between nonreinforced HMA pavement and other cases at 200 cycles of cyclic loading.

From Table 4.7 the reinforced HMA pavement with geogrid showed the greatest value of increased performances among new pavements. And, from Table 4.8 the nonreinforced PMA pavement showed the greatest value of increased performances among overlayed pavements. Therefore, geosynthetic and PM-AC is suitable for improving performance of new and overlayed pavement, respectively.

Table 4.7 Increased performances in new pavement when comparing with the nonreinforced HMA pavement

Type of pavement	Increased performances (%)
Nonreinfored PMA pavement	18.13
Reinforced HMA pavement with geogrid	39.50
Reinforced HMA pavement with geocomposite	7.59

Table 4.8 Increased performances in overlayed pavement when comparing with the nonreinforced HMA pavement

Type of pavement	Increased performances (%)
Nonreinfored PMA pavement	44.77
Reinforced HMA pavement with geogrid	43.46
Reinforced HMA pavement with geocomposite	38.37